

**NASA
Technical
Paper
2004**

April 1982

Investigation of Effects of Microphone Position and Orientation on Near-Ground Noise Measurements

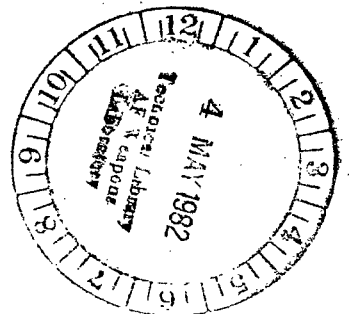
William L. Willshire, Jr.,
and Paul A. Nystrom

LOAN COPY: RETURN TO:
AFWL TECHNICAL LIBRARY
KIRTLAND AFB, N. M.

NASA
TP
2004
c.1



NASA





**NASA
Technical
Paper
2004**

1982

Investigation of Effects of Microphone Position and Orientation on Near-Ground Noise Measurements

William L. Willshire, Jr.,
and Paul A. Nystrom
*Langley Research Center
Hampton, Virginia*



National Aeronautics
and Space Administration

Scientific and Technical
Information Branch

SUMMARY

Three ground-level-microphone mounting techniques (flush mounting, inverting the microphone over a plate, and lying the microphone on a plate) were compared over a frequency range from 315 Hz to 20 kHz and over a wide range of incidence angles in the Langley Jet-Noise Laboratory anechoic room. The flush-mounted microphone, when compared with a free-field microphone, exhibited approximate pressure doubling up to a frequency of 10 kHz. Deviations from pressure doubling were attributed to the influence of diffraction from the plate. To minimize the influence of diffraction, the inverted and lying microphones were compared with the flush-mounted microphone. The inverted and lying microphones were in good agreement with the flush-mounted microphone at frequencies less than 4 kHz. All three microphone responses tended to have free-field response at near-grazing incidence. The free-field response at grazing incidence was attributed to the finite size of the plate used to simulate the ground surface. At frequencies less than 4 kHz, the inverted and lying 1/3-octave-band response spectra were fairly insensitive to the position of the microphone. At higher frequencies, the geometry of the microphone and its mounting became important. The inverted microphone 0.5 times the diameter above the plate gave the flattest response compared with the flush-mounted microphone. Nondimensional analysis of the inverted and lying results showed that for $kH \cos \theta < 0.7$ the response of the microphones approached that of the flush-mounted microphone.

INTRODUCTION

The purpose of this investigation was to compare the applicability of three ground-level-microphone mounting techniques to determining free-field noise source levels. The Federal Aviation Administration has established regulations and standard measurement procedures for aircraft noise certification (ref. 1). These procedures include using a standard microphone position 1.2 m (4 ft) above the ground. Microphones placed above a surface sense not only the direct acoustic signal from an aircraft but also a reflected aircraft signal from the surface. The reflected signal can either partially reinforce or cancel the direct signal, depending on the relative phase and magnitude of the signals. The combination of the direct and reflected signals results in an interference pattern. For a 1.2-m (4-ft) microphone, the first interference minimum occurs at a frequency less than 1 kHz.

The magnitude and phase of the reflected signal depend on several variables such as the characteristics of the noise source, the source position relative to the microphone, and the physical characteristics, including the ground impedance, of the reflecting surface. Unfortunately, the impedance of the ground surface varies greatly with changes of substance and is difficult to measure (ref. 2). Small variations in the height of the microphone can also induce errors into the measurements (ref. 3).

To overcome the interference-pattern problem associated with the 1.2-m (4-ft) microphone, higher and lower microphone positions are used. A commonly used higher position is 10 m (33 ft) above the ground (ref. 4). The higher position of the microphone in this configuration causes the first interference minimum to occur at a lower frequency than with the 1.2-m (4-ft) microphone. The 10-m (33-ft) position has an interference pattern associated with it, but 1/3-octave-band averaging of the more

closely spaced maxima and minima lessens the impact of the interference pattern on any particular 1/3-octave band of usual interest in jet-noise research. A variety of microphone positions near the ground have been proposed.

Of the near-ground microphone positions most often suggested, the flush-mounted position (ref. 5) is ideally the best, as it provides a pressure-doubled response at all frequencies and at all angles of incidence. However, the practical drawbacks of flush mounting cannot be ignored. It is not always feasible to flush mount a microphone, say to a paved surface, nor is it always easy to define the surface (e.g., areas covered by grass or gravel). To solve these problems, two other ground-level-microphone positioning techniques are usually proposed, one with the microphone lying on the surface (ref. 6) and the other with the microphone inverted above the surface (ref. 7). The surface can be either a ground board or the actual surface. In both cases, the microphone is assumed to be close enough to the surface and small enough to achieve pressure doubling at nearly all frequencies and at all angles of incidence.

The results of a laboratory experiment to compare three different ground-level-microphone mounting techniques are presented in this paper. The mounting techniques studied were flush mounting, lying the microphone on a plate, and inverting the microphone over a plate at various heights. A 12.7-mm (0.5-in.) microphone and a 10.2-cm (4.0-in.) midrange speaker were used in this investigation. The orientation between the source and the plate, used to simulate the ground, was varied over a wide range of incidence angles to simulate flyover noise measurements and ground-based noise measurements.

TEST FACILITY AND EQUIPMENT

Anechoic Room

The experiment was conducted in the anechoic room (fig. 1) in the Langley Jet-Noise Laboratory. The dimensions of the room, to the tips of the 0.6-m (2-ft) long glass fiber wedges, are 2.4 m (7.9 ft) × 3.1 m (10.2 ft) × 3.9 m (12.8 ft) for the height, width, and length, respectively. Except for the hardware used in the tests, there were no reflecting surfaces present in the room during the test. The acoustic properties of the room had previously been examined using a variable-frequency source. The room, without the test hardware, was found to exhibit an anechoic response (6-dB drop in sound pressure levels with a doubling of distance) for the frequency range of 150 Hz to 50 kHz.

Acoustic Source

The noise source (shown in the forefront of fig. 1) which was used for all the experiments was a 10.2-cm (4-in.) diameter unbaffled midrange speaker. The unbaffled speaker was selected over a baffled speaker and a tube point source. The construction of the unbaffled speaker minimized diffraction from the speaker itself, which resulted in a more uniform acoustic field than with the baffled speaker, particularly in the center of the acoustic field. The speaker also had an acceptable broadband frequency response and sufficient output power. The input signal to the speaker was broadband noise filtered to be within the frequency range of 315 Hz to 20 kHz. The source was positioned 1.8 m (6 ft) from the simulated ground surface.

Plate and Shroud

The plate which was used to simulate the ground surface can also be seen in figure 1. The plate is a 1.2 m (4 ft) square of aluminum, 6.4 mm (0.25 in.) thick. Attached to the plate in figure 1 are removable fiber-glass shrouds, shown in greater detail in figure 2. The shape of the shrouds were one-quarter ellipses with a 0.3-m (12-in.) major diameter and a 0.2-m (8-in.) minor diameter. The shrouds were 6.4 mm (0.25 in.) thick. The physical dimensions of the anechoic room necessitated the use of a finite-sized plate. Diffraction effects from the edges of the plate were anticipated. From earlier work (ref. 8), it was known that a rigid body with rounded edges would not exhibit as much diffraction as a rigid body with sharp edges. The shrouds were designed to minimize the diffraction from the edges of the plate by rounding the edges of the plate. Tests were performed both with and without this edge modification.

Plate Rotation

The variation in incidence angle was achieved by rotating the plate. Incidence angle θ is defined as the angle between the normal to the plate and the acoustic signal. The plate was mounted on a traversing mechanism so that the vertical centerline on the face of the plate would experience rotation without translation. (See fig. 3.) A digital stepping motor was used to rotate the plate in conjunction with a bidirectional totalizer to record its position. Measurement of the plate position was accurate and repeatable to within 0.5° over the entire range of angles tested. A laser was used to align the speaker with the plate.

Microphone and Orientation

The same microphone was used for all the experiments to eliminate any errors that might be introduced by characteristic differences between individual microphones. The microphone used was a 12.7-mm (0.5-in.) diameter condenser microphone, factory adjusted to be a pressure microphone. The microphone was tested in four different configurations: flush mounted to the plate (fig. 4(a)), lying on the plate (fig. 4(b)), inverted over the plate at various heights (fig. 4(c)), and free field at the same spatial location but with the plate removed. At all angles of incidence of the plate to the source, the microphone was at grazing incidence to the source for the lying and free-field microphone configurations. The stand which held the microphone in the inverted position can be seen in figure 4(c). The sensitivity of the microphone was regularly measured at 250 Hz using an oscillating piston-type calibrator. The microphone calibration was used in the reduction of the data to eliminate any variations that could have been caused by changes in the sensitivity of the microphone. The maximum sensitivity correction was less than 0.5 dB.

Signal Analysis

The output signal from the microphone was analyzed using simultaneous 1/3-octave-band filters with center frequencies ranging from 315 Hz to 20 kHz and a 16-second averaging time. The coefficient of variation, the ratio of the random statistical error to the average measured pressure, is estimated to be 0.03 for the lowest frequency band and decreases for higher frequency bands. The attenuation of each of the 19 filters was regularly measured and was included in the data acquisition to

adjust the levels in each of the bands before they were recorded. The filter-attenuation corrections were accurate to within 0.25 dB and varied only slightly from day to day.

Ambient Condition

Along with the acoustic data gathered for each configuration, the ambient temperature, pressure, and relative humidity were measured and recorded. The temperature was measured using a thermistor, accurate to within 1°C (1.8°F); the ambient pressure was measured with an absolute barometer, accurate to within 1 mm Hg (0.04 in. Hg); and the relative humidity was measured with a digital hygrometer, accurate to within 1 percent.

TEST CONDITIONS AND PROCEDURES

The test matrix is illustrated in table I. Most of the experiments were conducted with the plate edge treatment (shrouds) and without the microphone grid cap. However, some tests were performed with the microphone grid cap on. The grid cap was found to have little effect at any frequency or at any angle of incidence. To insure that the different microphone mounting configurations were as similar as possible (the flush-mounted microphone could not be used with a grid cap), data to be presented in this report were taken without the microphone grid cap. The three ground-level mounting techniques were tested at 23 incidence angles, -20° to 90°, in 5° increments. The negative incidence angles were included to check the symmetry and repeatability of the results. The microphone in the inverted configuration was tested at heights above the plate of 0.125, 0.25, 0.50, 0.75, 1, and 2 times the microphone diameter (12.7 mm (0.5 in.)). A free-field test was also conducted with the plate removed and the microphone at grazing incidence.

Each run was begun by configuring the plate in accordance with the test condition (with or without the edge treatment). When the shrouds were used, the junction between the edges of the plate and the shrouds was smooth. A laser was used to insure that the speaker face and the plate were parallel and that the speaker was pointed toward the center of the plate. The plate was then rotated and the alignment checked. The microphone was calibrated using a piston-type precision sound source, and the attenuation of the 1/3-octave-band filters was measured and recorded. The microphone was mounted on the plate in accordance with the test conditions. The time and atmospheric data were measured, and the acquisition of the 1/3-octave-band data was initiated. Before the acoustic data were stored, the 1/3-octave-band filter-attenuation corrections were applied. A new incidence angle was then chosen, and the above process was repeated.

DATA ANALYSIS

The basic results of the experiment were 1/3-octave-band spectra of the acoustic source for the various microphone mounting techniques. To compare the frequency response of the different mounting techniques, the measured spectra were compared with common reference spectra. An obvious first choice for the reference spectrum was the free-field 1/3-octave-band spectrum, but for reasons mentioned in the following paragraph another reference spectrum was selected.

The finite size of the plate used to simulate the ground surface gave rise to concerns about the diffraction from the plate edges influencing the comparison of the different microphone mounting techniques. Two approaches were used to minimize the effect of diffraction. The first was the use of the shrouds, discussed previously. The second was the careful selection of the reference spectra used in the data analysis. The reference spectra chosen to compare with the inverted- and lying-microphone data were the flush-mounted-microphone data at the same incidence angle. With equal incidence angles, the geometry between the source and the plate, and therefore the edge diffraction effects, would be identical for the two spectra. Use of reference data at matched incidence angles in the analysis is referred to as using a matched reference.

RESULTS AND DISCUSSION

Data Presentation Format

The typical format that is used to illustrate the frequency response of the various microphone mounting techniques is shown in figure 5. The ordinate is relative sound pressure level in dB and the abscissa is frequency in Hz. The legend and the key in figure 5 identify the data presented. In this case the data are for the flush-mounted microphone without the edge treatment (shrouds), using the free-field microphone as the reference microphone. Data are given for 10 incidence angles, and the reference data used were for the free-field microphone at grazing incidence. Ambient conditions for the measured data are given in table II.

Effect of Plate-Edge Treatment

Figures 5 and 6 show the effect that the shrouds have on the response spectra. Both figures are comparisons of a flush-mounted microphone with the free-field microphone. Figure 5 is without the shrouds, and figure 6 is with the shrouds. The shrouds tend to flatten the spectra, especially near the midrange 1/3-octave bands. The shrouds round off the edges of the plate and appear to make the diffraction caused by the plate tend toward that of an infinite surface much faster than the associated increase in the projected area of the plate with the shrouds. The effect of the shrouds is a reduction of the influence of diffraction in the measured results. The remainder of the data presented are with the plate-edge treatment.

Measurement Repeatability

As a test of repeatability and symmetry of the experiment (with respect to the angle of incidence), the flush-mounted microphone was tested twice. Figure 7 shows a comparison of the two tests. The agreement is within the experimental error (± 1 dB) from one test to another and in positive angles to negative angles.

Effect of Matched Reference

The effect of a matched reference to minimize the influence of diffraction is shown in figures 8 and 9. Results are given in the figures for an inverted microphone 1 diameter above the plate. The reference microphone for the results given in figure 8 was the flush-mounted microphone at 0° incidence angle. The reference for

the results in figure 9 was also the flush-mounted-microphone data, but the comparison was made between data of equal incidence angle. The results using the matched reference more clearly exhibit the expected systematic deviation, increasing with incidence angle, of the inverted response from the flush response at higher frequencies than do the 0° reference results.

In figure 8, the low-frequency data for the 80° and 85° incidence angles do not cluster around the zero line like the results at smaller incidence angles. The reason for this difference at large incidence angles is that at grazing incidence and low frequency the diffraction around a flat object has been shown to be small, and the response of a microphone near the surface of the object has been shown to approach the free-field response (ref. 9). Similar response is expected for the rectangular plate used to simulate the ground in the present experiment.

The results given in this report represent the difference between two spectra, a measurement spectrum from a particular microphone configuration and a reference spectrum. For the results given in figure 8, the reference spectrum was not influenced by the tendency toward free-field response, because the plate was at normal incidence when the spectrum was obtained. The measurement spectrum from the inverted microphone was influenced by the tendency toward free-field response at grazing incidence. When the difference between the two spectra was taken to get the results given in figure 9, the tendency toward the free-field response was incorporated in the results. When both spectra being compared have equal incidence angles, as in figure 10, the tendency toward free-field response is in both spectra and is subtracted from the results.

The high-frequency dips in figures 8 and 9 are due to the microphone being placed above the plate. The inverted microphone senses a direct signal and a reflected signal. For frequencies less than 4 kHz, the path-length difference between the two signals is a small portion of a wavelength, and the inverted response is essentially that of the flush-mounted microphone. For higher frequencies the path-length difference becomes significant, and destructive interference between the two signals develops. The dip in the frequency response shifts to higher frequencies as the path-length difference decreases with increasing incidence angle. Matched references have been used to compute the results given in the remainder of this report.

Results for Flush-Mounted Microphone

The flush-mounted microphone at various angles of incidence was compared with the free-field microphone. The results are shown in figure 6. For incidence angles up to 70°, the relative sound pressure level (SPL) up to a frequency of 10 kHz is nearly 6 dB, indicating pressure doubling. Deviations from pressure doubling are caused by the diffraction of the sound field by the plate. At near-grazing incidence (an incidence angle approaching 90°), the response tends to be as if it were in the free field. The same tendency toward free-field response at large incidence angles was observed when the inverted microphone was compared with the flush-mounted microphone (fig. 8). Even though both configurations show the same trend when compared with the free-field microphone, a conclusion as to whether the tendency toward free-field response occurs at high incidence angles for a microphone positioned over a larger surface (the ground) cannot be drawn because of the size of the plate used in the experiment. Microphone responses for the inverted and lying mounting techniques are computed using the flush-mounted microphone at the same incidence angle.

Results for Inverted Microphone

The results for the inverted microphone with the matched flush microphone as the reference are shown in figure 9 for a height-to-diameter ratio (H/D) of 1.0. The laboratory results shown in figure 9 show excellent agreement with the flush-mounted microphone for frequencies less than 4 kHz. For higher frequencies, there is a systematic deviation which occurs as a function of incidence angle. As previously discussed, the dips are due to destructive interference between the direct signals and the reflected signals, and the frequency shift of the dip is caused by the changing geometry, which is caused by the different incidence angles.

The results of a systematic variation of microphone heights for the inverted mounting technique are shown in figures 10 through 14 for $H/D = 2, 0.75, 0.50, 0.25,$ and $0.125,$ respectively. For frequencies less than 4 kHz (1 kHz for the $H/D = 2$ curves), the inverted-microphone responses are in good agreement with the flush-mounted-microphone responses. At the higher frequencies, there is again a strong geometric dependency. As the microphone is positioned higher above the plate, the destructive-interference dip is moved to lower frequencies because of longer path-length differences. The closer microphones ($H/D = 0.25$ and 0.125 (figs. 13 and 14)) have humps at about 16 kHz caused by some constructive interference which is not a strong function of incidence angle. The constructive interference is possibly due to some resonance involving the microphone stand or the microphone itself.

Results for Lying Microphone

The results for the configuration with the microphone lying on the plate compared with the matched flush-mounted microphone are given in figure 15. The lying-microphone response is fairly flat up to about 4 kHz. Above 4 kHz, a strong angle dependency is observed.

Of the inverted and lying configurations tested, the response of the inverted microphone 0.5 times the diameter above the plate (fig. 12) was the closest to the response of the flush-mounted microphone. The destructive-interference dip is greater than 10 kHz in frequency and is partially offset by the constructive interference mentioned in the section "Results for Inverted Microphone."

Comparison of Mounting Techniques

To directly compare the different microphone-mounting techniques at various angles of incidence, a series of cross plots were made grouping the frequency responses according to incidence angle. The results are given in figures 16 through 24 corresponding to the incidence angles of $0^\circ, 10^\circ, 20^\circ, 30^\circ, 60^\circ, 70^\circ, 75^\circ, 80^\circ,$ and $85^\circ,$ respectively. At normal incidence there are large differences in the spectra between different microphone mounting techniques. The responses are fairly flat to about 1 kHz (4 kHz excluding the $H/D = 2$ case), after which the height-dependent dips show up. At the intermediate angles (30° and 60°), the curves tend to flatten as the dips move up in frequency. At near-grazing incidence (80° and above), the curves are generally flat up to about 10 kHz. The results at higher frequencies for the inverted configurations where $H/D = 0.25$ and 0.50 exhibit constructive-interference bumps.

Blurring of the location of the minima by the 1/3-octave-band averaging is illustrated in figure 16. In this figure, the first minimum for the $H/D = 2$ case

occurs at a frequency of 4 kHz. Since all the data in the figure are for the same incidence angle (0°), the first minimum for the $H/D = 1$ case would be expected to be at 8 kHz. However, because of the 1/3-octave-band frequency resolution, the minimum occurs at a higher frequency.

Nondimensional Analysis

The results from the inverted configurations were replotted against the non-dimensional parameter $kH \cos \theta$, where k is the wave number, H is the microphone height above the plate, and θ is incidence angle. The results are given in figures 25 through 30 for the inverted configurations, with $H/D = 2, 1, 0.75, 0.50, 0.25,$ and $0.125,$ respectively. Similar results are given in figure 31 for the lying configuration, where a value of one-half of the microphone diameter was used for the parameter H . The dips observed previously which were a function of incidence angle for a particular configuration are independent of incidence angle in this presentation format. The location of the first minima between the configurations is roughly the same, between $kH \cos \theta = 1$ and $kH \cos \theta = 3$. The minima do not fall exactly on top of one another because of the 1/3-octave-band averaging. In the figures, the grazing-incidence results deviate from the normal incidence angle results, particularly for larger values of $kH \cos \theta$.

For the inverted configurations where $H/D = 0.25$ and 0.125 (figs. 29 and 30), the results at large incidence angles do not agree with the results at smaller incidence angles. This indicates that these results are influenced by a phenomenon, perhaps a resonance caused by the microphone stand, which is not a simple function of $kH \cos \theta$. For the inverted and lying configurations tested, a response close to that of the flush-mounted microphone was achieved with $kH \cos \theta < 0.7$. There were deviations from this response at grazing incidence.

CONCLUDING REMARKS

Three ground-level-microphone mounting techniques were compared over a frequency range from 315 Hz to 20 kHz and over a wide range of incidence angles θ in the Langley Jet-Noise Laboratory anechoic room. The techniques, tested with a 12.7-mm (0.5-in.) microphone, were flush mounting, lying the microphone on a plate, and inverting the microphone over a plate. The inverted case was tested at six heights H , ranging from 0.125 to 2 times the microphone diameter D above the plate. The flush-mounted response was 6 dB greater than the free-field response up to 10 kHz, indicating pressure doubling. Deviations from pressure doubling of the flush-mounted response were caused by diffraction of the sound field by the plate. The lying- and inverted-microphone frequency responses less than 4 kHz were in good agreement with the flush-mounted-microphone response (1 kHz for the $H/D = 2$ case). At higher frequencies, interference dips were observed which were strong functions of incidence angle and of microphone height above the plate. When the inverted and lying results were replotted against the nondimensional parameter $kH \cos \theta$, where k is the wave number, the dips observed in the responses collapsed around a common curve, and the results were independent of configuration and incidence angle. For $kH \cos \theta < 0.7$, the responses of the inverted and lying configurations approached that of the flush-mounted microphone.

At near-grazing incidence, all three mounting techniques tended to have free-field response. This tendency toward free-field response was attributed to the finite size of the plate used to simulate the ground surface. A constructive

interference was observed at high frequencies with the inverted configurations for $H/D = 0.25$ and $H/D = 0.125$. The amplification was not a strong function of incidence angle and may have been caused by a resonance involving the microphone stand or the microphone itself. The ground-level-microphone mounting technique which was the closest to the flush-mounted-microphone results was the inverted microphone positioned 0.5 times the diameter above the plate.

Langley Research Center
National Aeronautics and Space Administration
Hampton, VA 23665
March 18, 1982

REFERENCES

1. Noise Standards: Aircraft Type and Airworthiness Certification. Federal Aviation Regulations, vol. III, pt. 36, FAA, 1978.
2. Oncley, Paul B.: Review of Theory and Methods for the Prediction of Ground Effects on Aircraft Noise Propagation. AIAA Paper 75-538, Mar. 1975.
3. Pernet, D. F.; and Payne, R. C.: The Effect of Small Variations in the Height of a Microphone Above Ground Surface on the Measurement of Aircraft Noise. NPL Acoustics Rep. Ac 77, British A.R.C., Oct. 1976.
4. Smith, M. J. T.: International Aircraft Noise Measurement Procedures - Expensive Acquisition of Poor Quality Data. AIAA Paper 77-1371, Oct. 1977.
5. Taniguchi, H. H.; and Rasmussen, G.: Selection and Use of Microphones for Engine and Aircraft Noise Measurements. Sound & Vib., vol. 13, no. 2, Feb. 1979, pp. 12-20.
6. Piercy, J. E.; and Embleton, T. F. W.: Effect of Ground on Near-Horizontal Sound Propagation. Reprint 740211, Soc. Automot. Eng., 1974.
7. McKaig, Merle B.: Use of Flush-Mounted Microphones To Acquire Free-Field Data. AIAA Paper No. 74-92, Jan.-Feb. 1974.
8. Norum, Thomas D.; and Seiner, John M.: Shape Optimization of Pressure Gradient Microphones. NASA TM-78632, 1977.
9. Maciulaitis, Algirdas; Seiner, John M.; and Norum, Thomas D.: Sound Scattering by Rigid Oblate Spheroids, With Implication to Pressure Gradient Microphones. NASA TN D-8140, 1976.

SYMBOLS

D	microphone diameter, mm (in.)
H	microphone height, mm (in.)
k	wave number
p	barometric pressure, mm Hg (in. Hg)
RH	relative humidity, percent
SPL	sound pressure level
T	temperature, °C (°F)
θ	incidence angle, deg

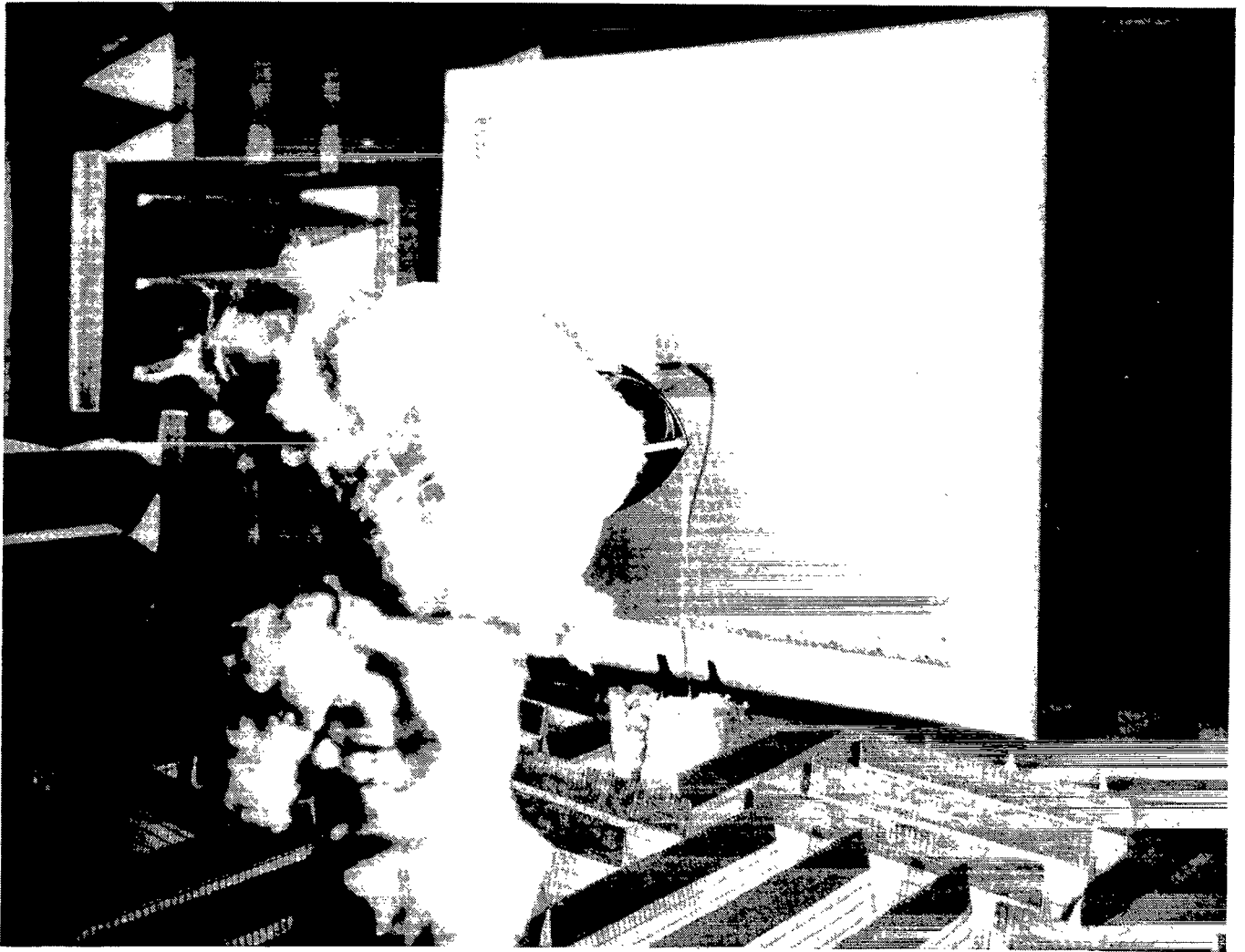
TABLE I.- TEST MATRIX

Position ¹	Shrouds		Grid cap	
	With	Without	With	Without
Flush	X	X		X
Free field				X
Inverted; H/D = 2	X			X
Inverted; H/D = 1	X		X	X
Inverted; H/D = 0.75	X			X
Inverted; H/D = 0.50	X			X
Inverted; H/D = 0.25	X			X
Inverted; H/D = 0.125	X			X
Lying	X			X

¹Every position was tested at 23 incidence angles from -20° to 90° in 5° increments and at frequencies from 315 Hz to 20 kHz.

TABLE II.- TEST AMBIENT CONDITIONS

Position	T		P		RH, percent
	°C	°F	mm Hg	in. Hg	
Flush without shrouds	27	81	760	29.9	77
Flush with shrouds	27	81	757	29.8	71
Free field	28	82	757	29.8	53
Inverted; H/D = 2	30	86	757	29.8	60
Inverted; H/D = 1	31	88	757	29.8	56
Inverted; H/D = 0.75	28	82	758	29.8	60
Inverted; H/D = 0.50	28	82	758	29.8	59
Inverted; H/D = 0.25	28	82	758	29.8	57
Inverted; H/D = 0.125	28	82	757	29.8	52
Lying	27	81	757	29.8	54



L-79-6959

Figure 1.- Experimental setup.

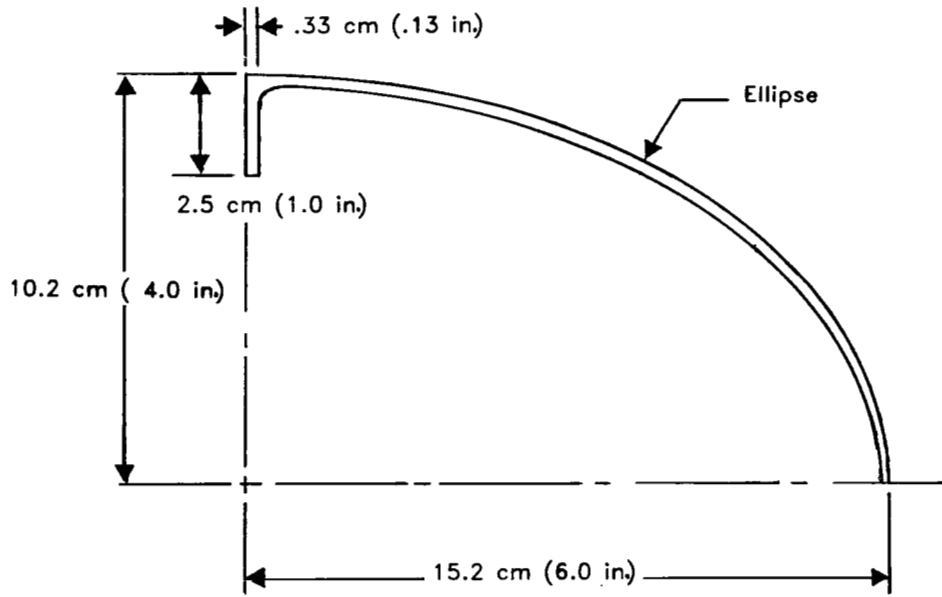


Figure 2.- Shape of edge treatment shrouds.

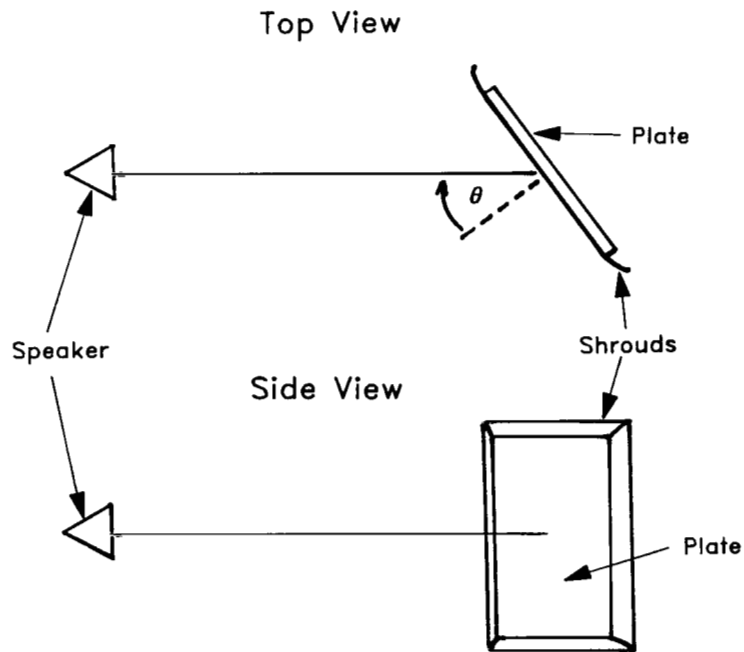
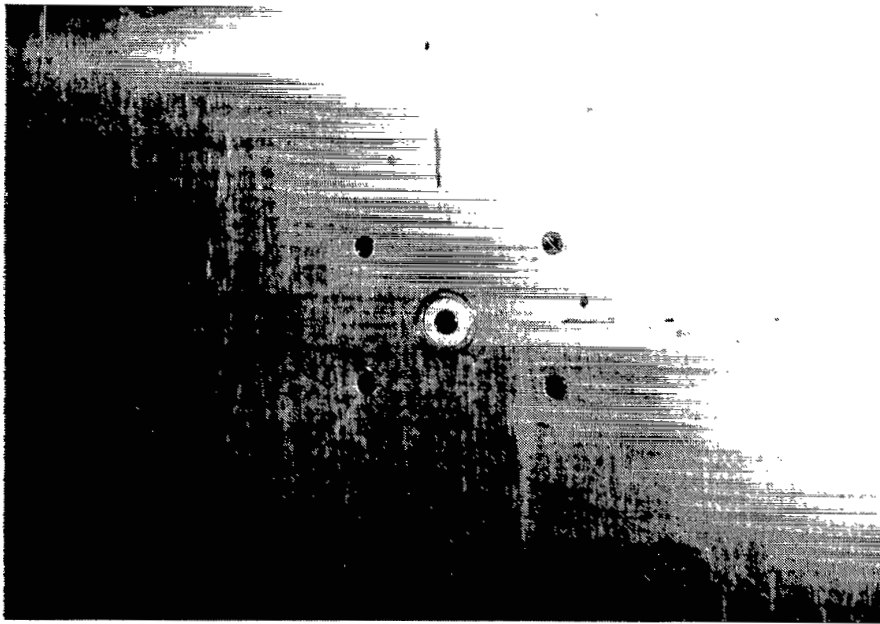
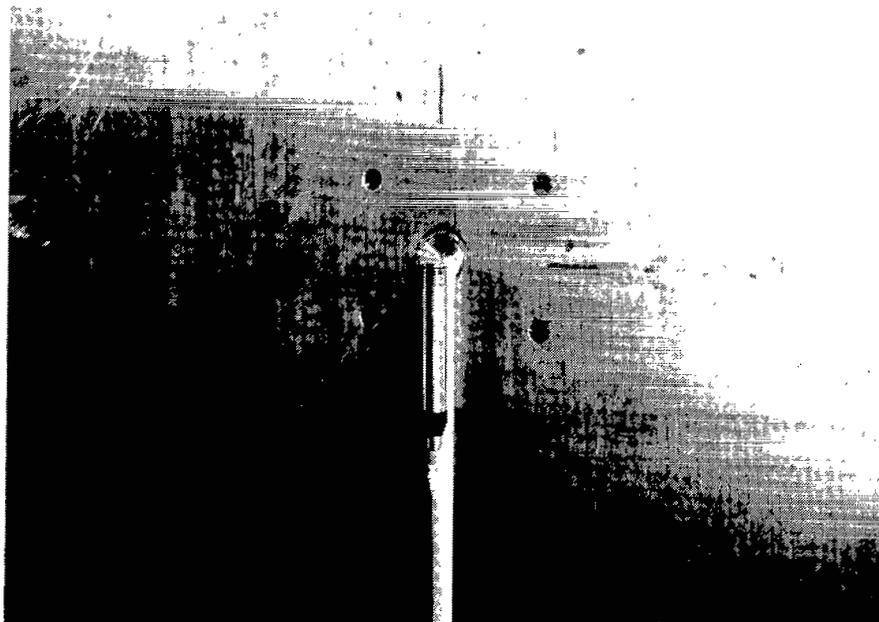


Figure 3.- Plate rotation geometry.



L-79-6964

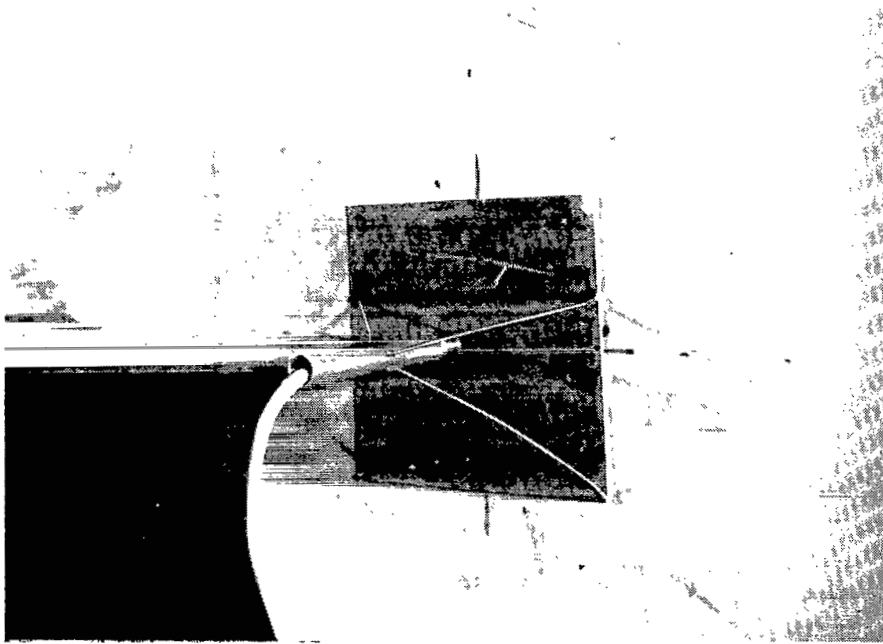
(a) Flush mounted.



L-79-6961

(b) Lying on plate.

Figure 4.- Microphone configurations.



L-79-6962

(c) Inverted over plate.

Figure 4.- Concluded.

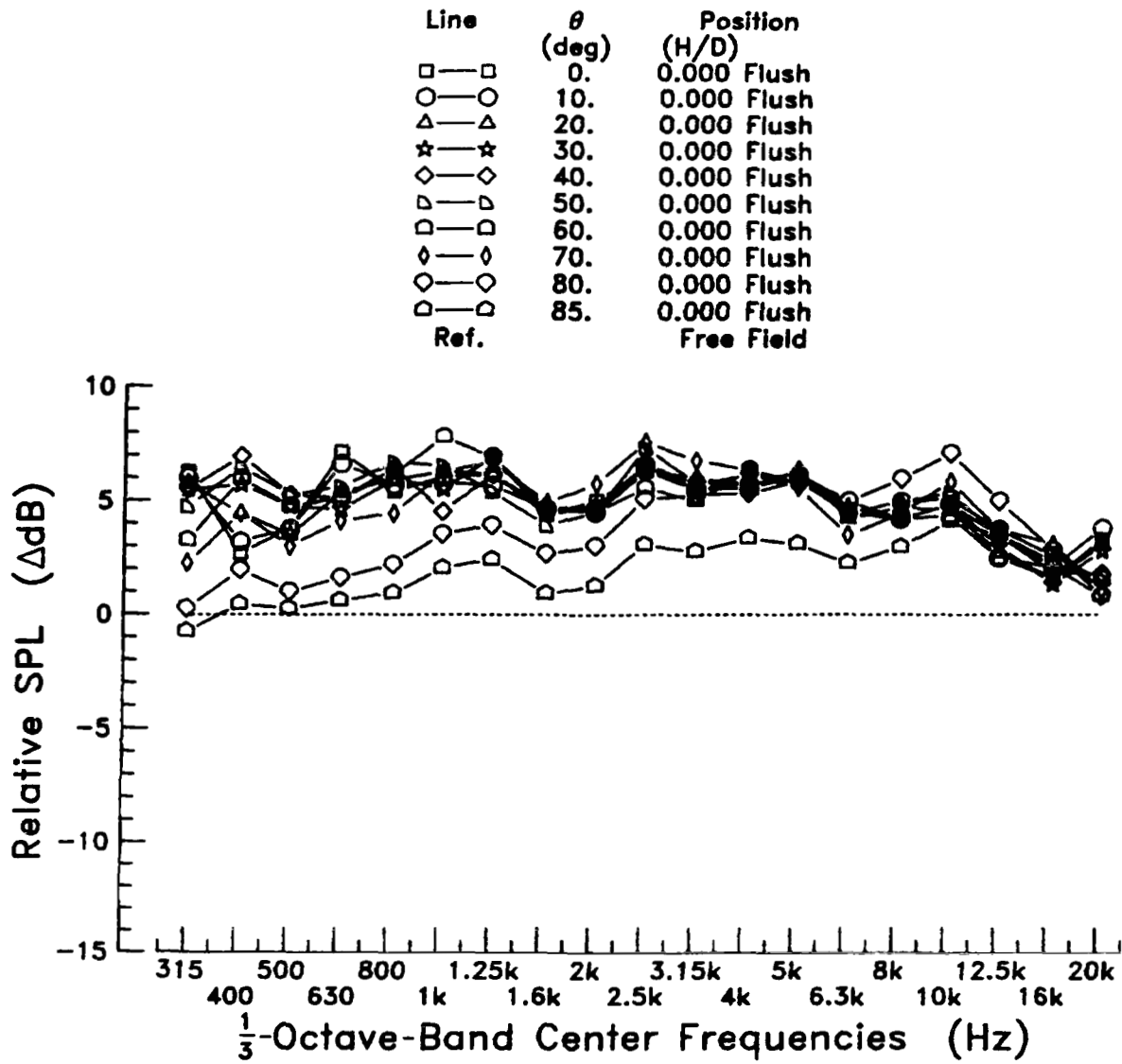


Figure 5.- Flush-mounted microphone without shrouds versus free-field microphone.

Line	θ (deg)	Position (H/D)
□—□	0.	0.000 Flush
○—○	10.	0.000 Flush
△—△	20.	0.000 Flush
☆—☆	30.	0.000 Flush
◇—◇	40.	0.000 Flush
▷—▷	50.	0.000 Flush
◻—◻	60.	0.000 Flush
◊—◊	70.	0.000 Flush
○—○	80.	0.000 Flush
◻—◻	85.	0.000 Flush
Ref.		Free Field

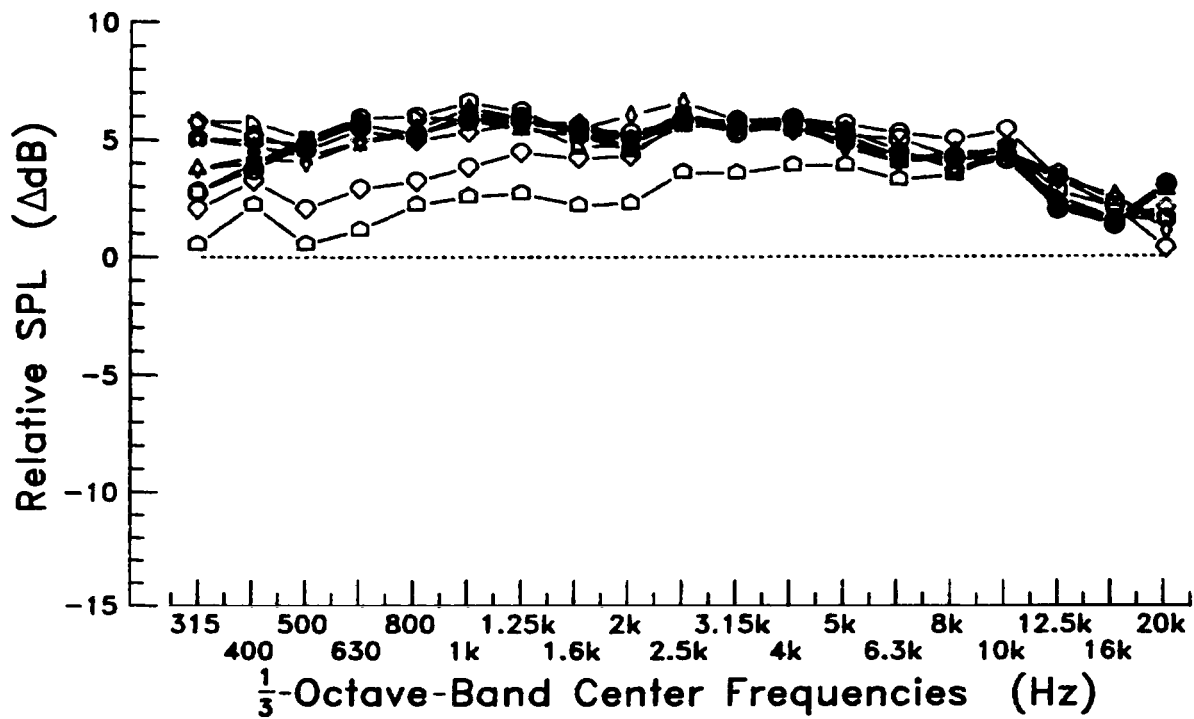


Figure 6.- Flush-mounted microphone with shrouds versus free-field microphone.

Line	θ (deg)	Position (H/D)
□—□	-20.	0.000 Flush
○—○	-15.	0.000 Flush
△—△	-10.	0.000 Flush
☆—☆	-5.	0.000 Flush
◇—◇	5.	0.000 Flush
▷—▷	10.	0.000 Flush
◻—◻	15.	0.000 Flush
◊—◊	20.	0.000 Flush
Ref.	Match	0.000 Flush

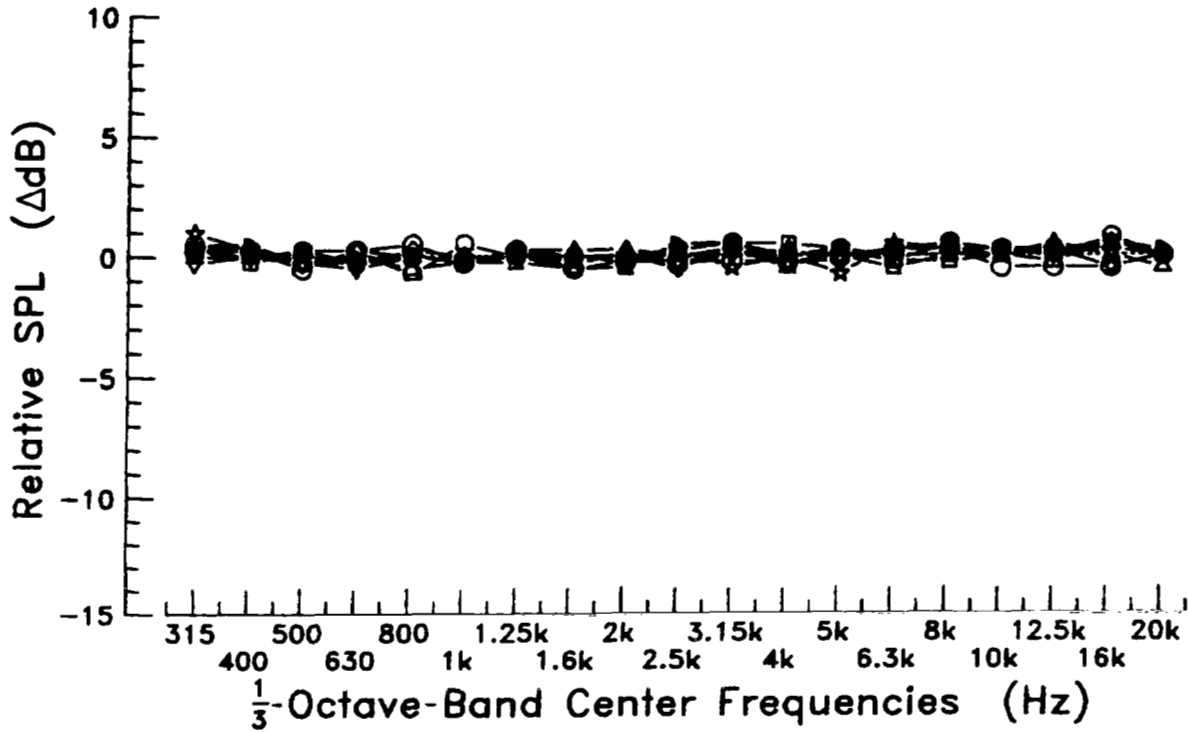


Figure 7.- Repeatability tests for flush-mounted microphone.

Line	θ (deg)	Position (H/D)
□—□	0.	1.000 Inverted
○—○	10.	1.000 Inverted
△—△	20.	1.000 Inverted
☆—☆	30.	1.000 Inverted
◇—◇	40.	1.000 Inverted
▷—▷	50.	1.000 Inverted
◻—◻	60.	1.000 Inverted
◊—◊	70.	1.000 Inverted
○—○	80.	1.000 Inverted
▷—▷	85.	1.000 Inverted
Ref.	0.	0.000 Flush

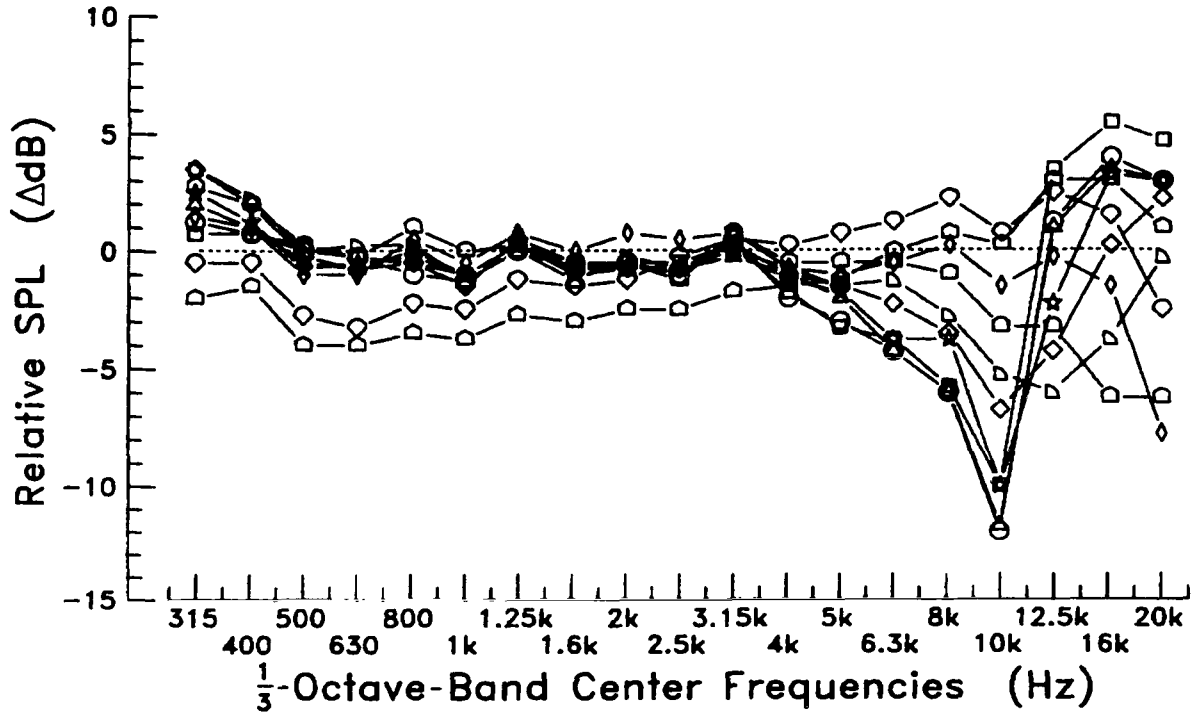


Figure 8.- Inverted microphone for H/D = 1 versus flush-mounted microphone at 0° reference.

Line	θ (deg)	Position (H/D)
□—□	0.	1.000 Inverted
○—○	10.	1.000 Inverted
△—△	20.	1.000 Inverted
☆—☆	30.	1.000 Inverted
◇—◇	40.	1.000 Inverted
▷—▷	50.	1.000 Inverted
◻—◻	60.	1.000 Inverted
◊—◊	70.	1.000 Inverted
◈—◈	80.	1.000 Inverted
◑—◑	85.	1.000 Inverted
Ref.	Match	0.000 Flush

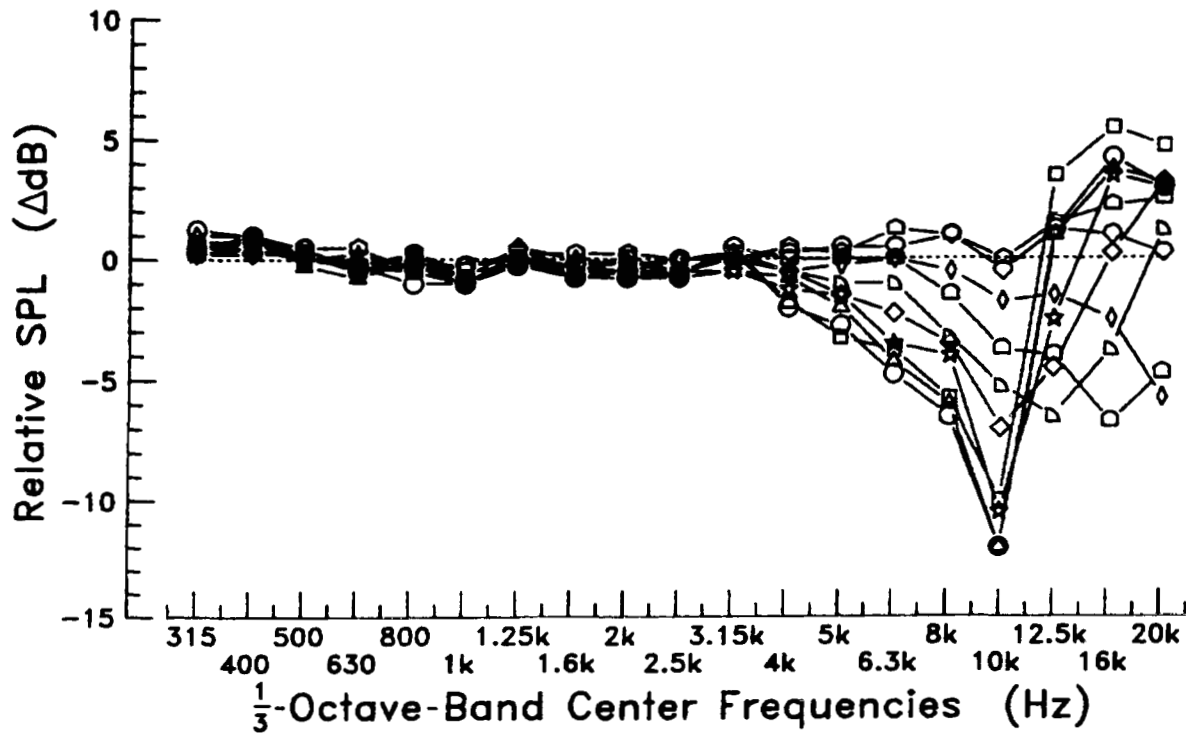


Figure 9.- Inverted microphone for $H/D = 1$ versus flush-mounted microphone.

Line	θ (deg)	Position (H/D)
□—□	0.	2.000 Inverted
○—○	10.	2.000 Inverted
△—△	20.	2.000 Inverted
☆—☆	30.	2.000 Inverted
◇—◇	40.	2.000 Inverted
▷—▷	50.	2.000 Inverted
◻—◻	60.	2.000 Inverted
◊—◊	70.	2.000 Inverted
◌—◌	80.	2.000 Inverted
◑—◑	85.	2.000 Inverted
Ref.	Match	0.000 Flush

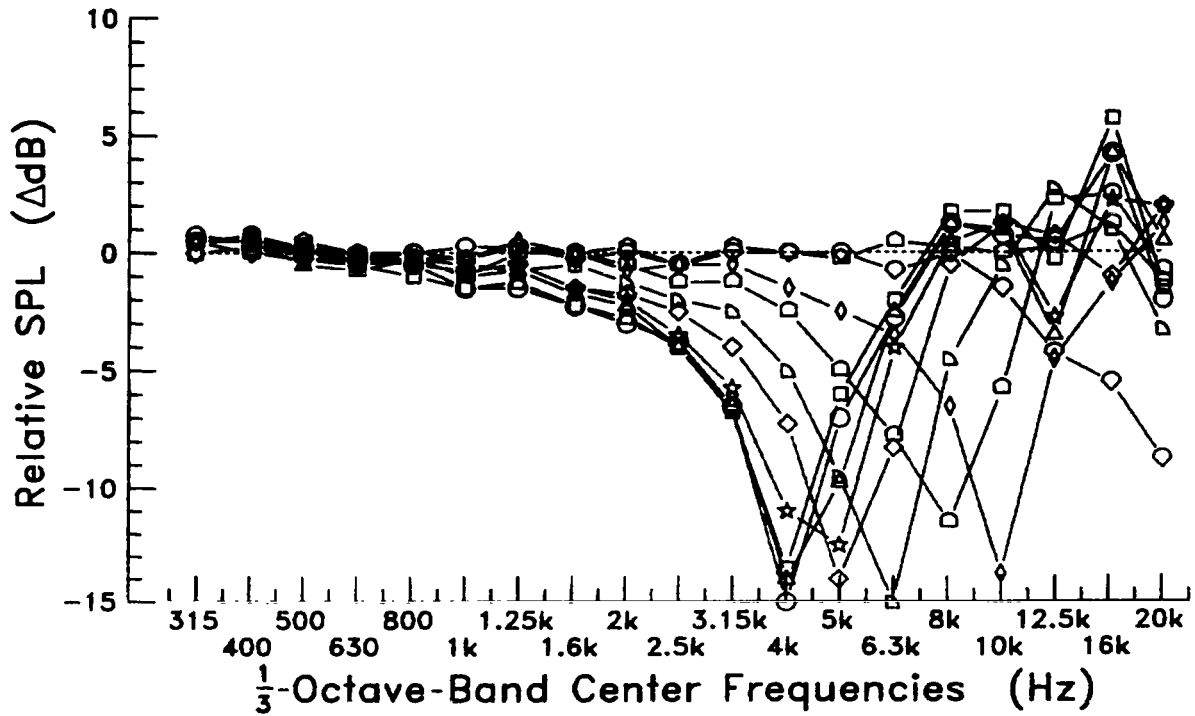


Figure 10.- Inverted microphone for H/D = 2 versus flush-mounted microphone.

Line	θ (deg)	Position (H/D)
□—□	0.	0.750 Inverted
○—○	10.	0.750 Inverted
△—△	20.	0.750 Inverted
☆—☆	30.	0.750 Inverted
◇—◇	40.	0.750 Inverted
▷—▷	50.	0.750 Inverted
◻—◻	60.	0.750 Inverted
◊—◊	70.	0.750 Inverted
◌—◌	80.	0.750 Inverted
◍—◍	85.	0.750 Inverted
Ref.	Match	0.000 Flush

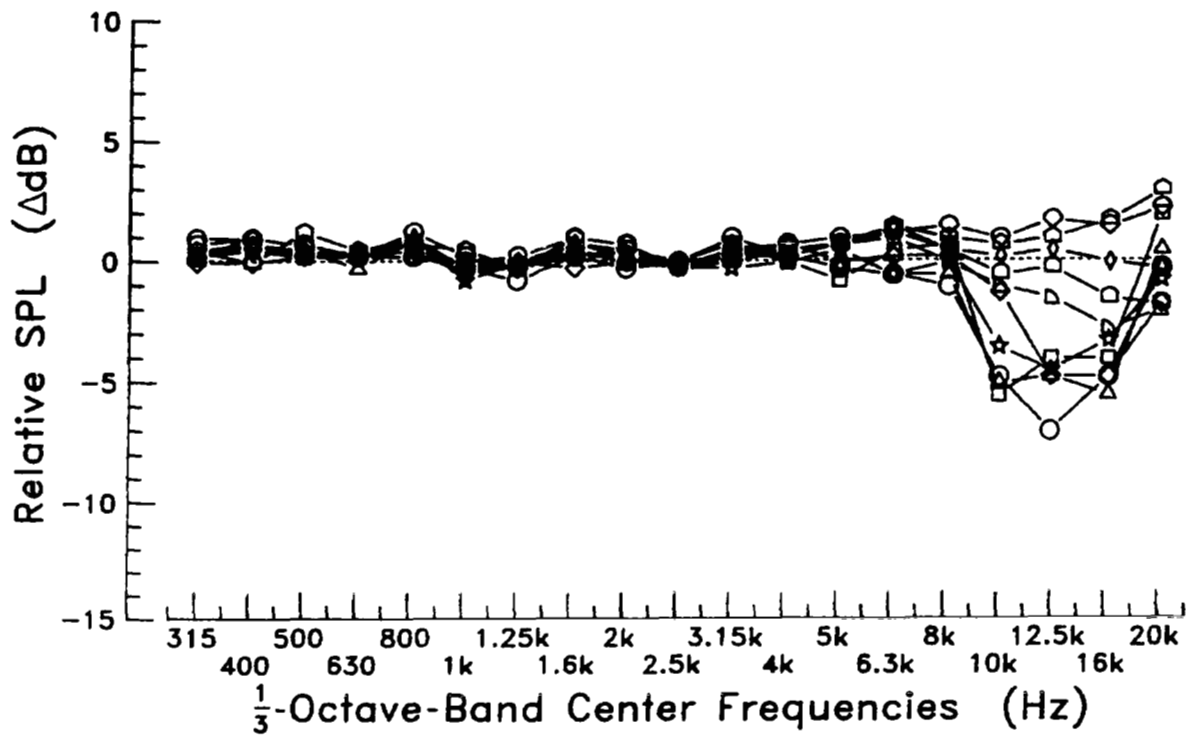


Figure 11.- Inverted microphone for H/D = 0.75 versus flush-mounted microphone.

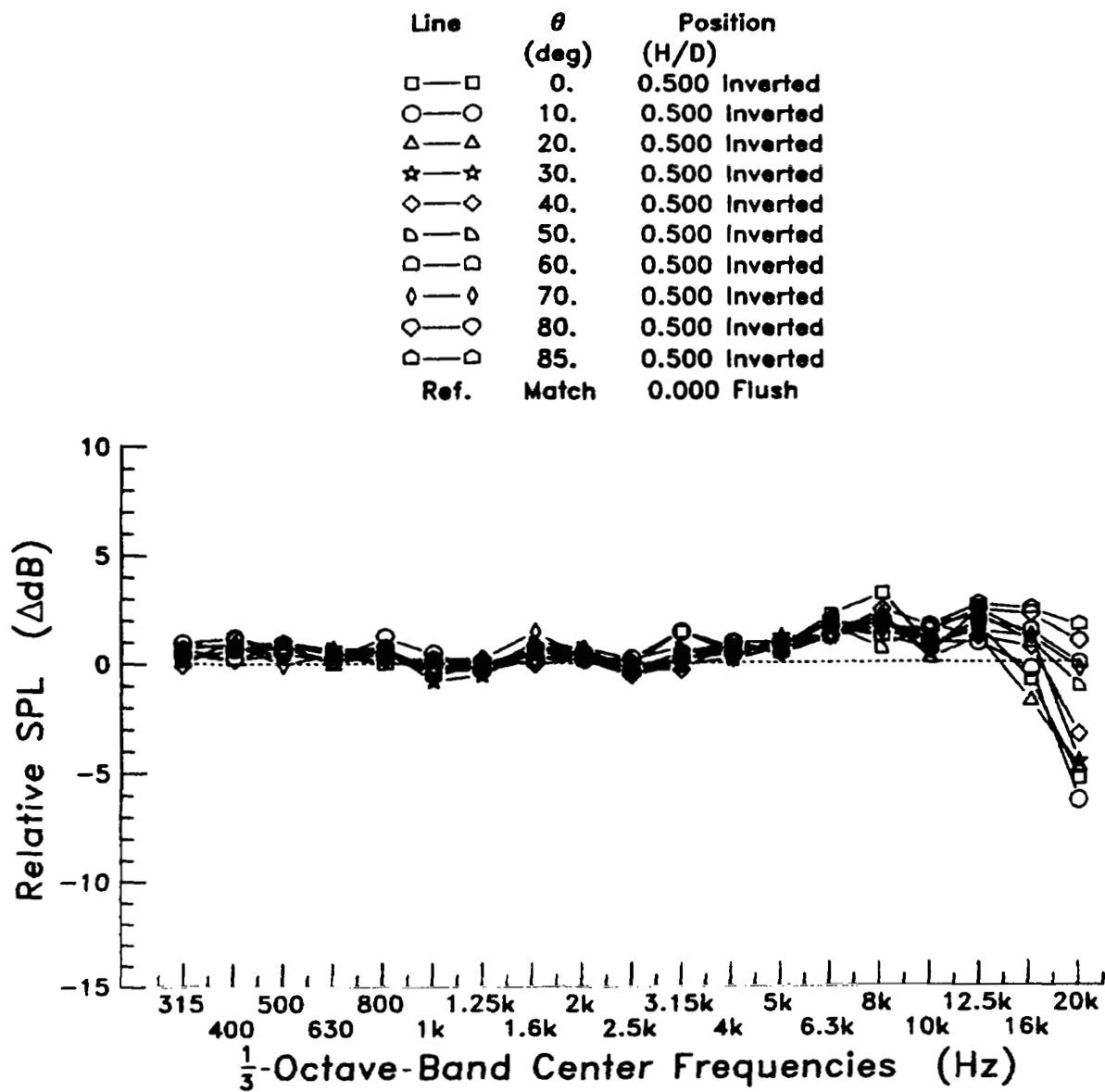


Figure 12.- Inverted microphone for H/D = 0.50 versus flush-mounted microphone.

Line	θ (deg)	Position (H/D)
□—□	0.	0.250 Inverted
○—○	10.	0.250 Inverted
△—△	20.	0.250 Inverted
☆—☆	30.	0.250 Inverted
◇—◇	40.	0.250 Inverted
▷—▷	50.	0.250 Inverted
◻—◻	60.	0.250 Inverted
◊—◊	70.	0.250 Inverted
◌—◌	80.	0.250 Inverted
◐—◐	85.	0.250 Inverted
Ref.	Match	0.000 Flush

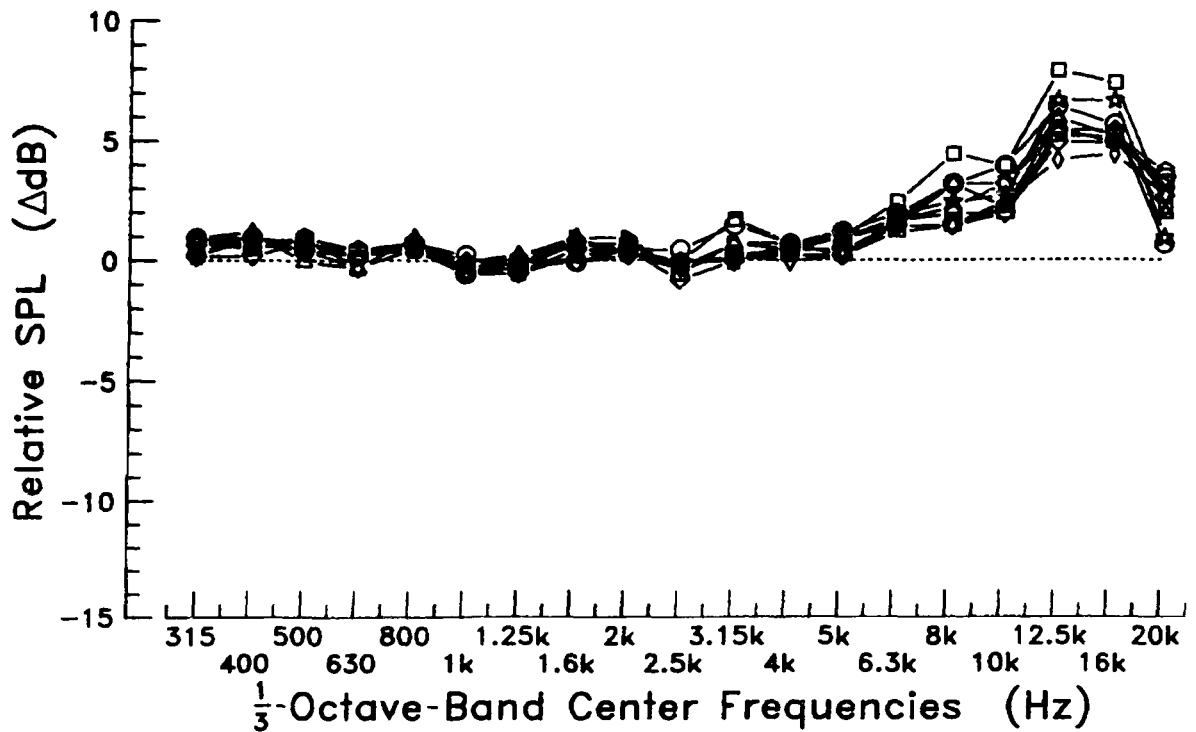


Figure 13.- Inverted microphone for $H/D = 0.25$ versus flush-mounted microphone.

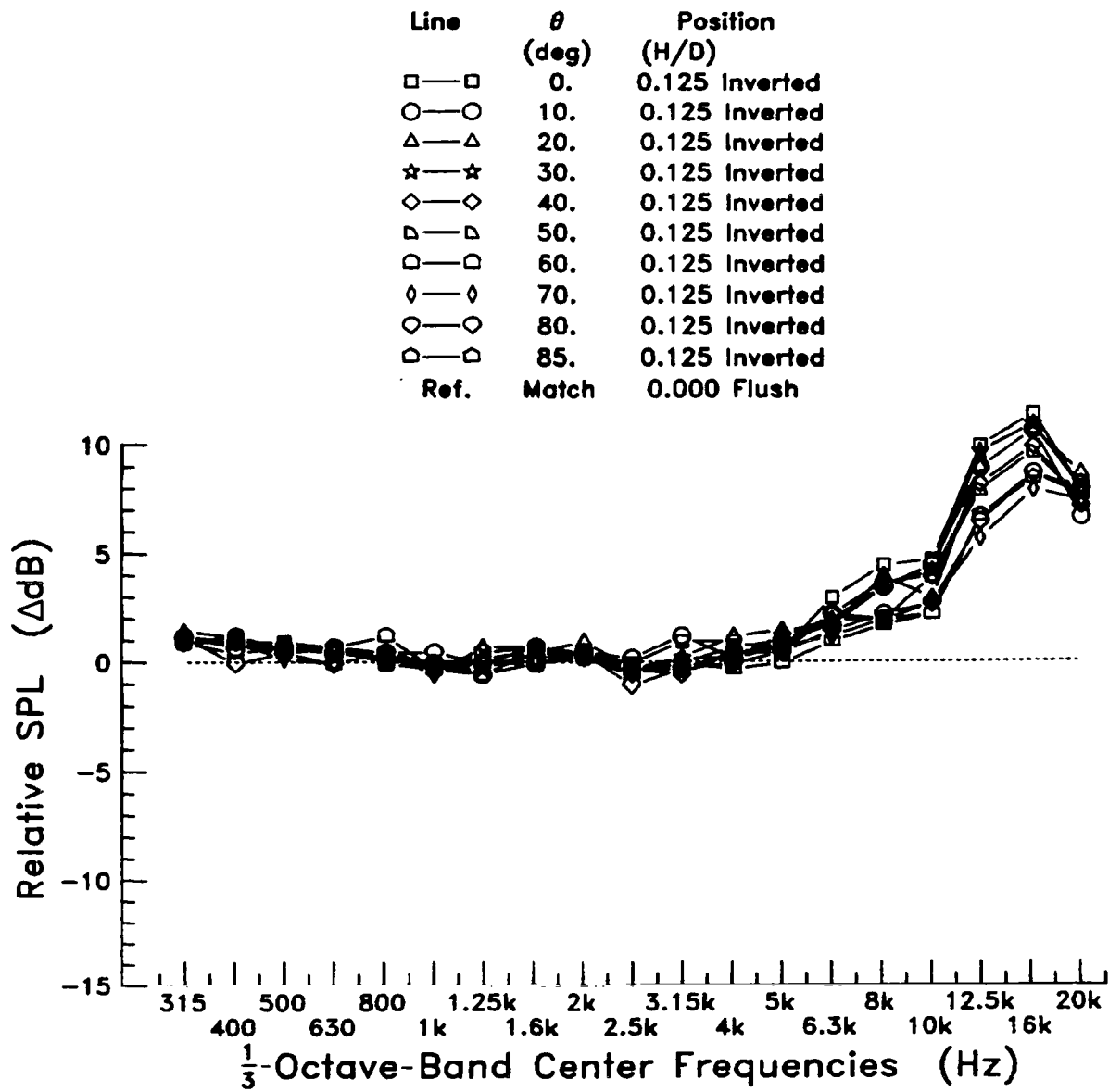


Figure 14.- Inverted microphone for $H/D = 0.125$ versus flush-mounted microphone.

Line	θ (deg)	Position (H/D)
□—□	0.	0.500 Lying
○—○	10.	0.500 Lying
△—△	20.	0.500 Lying
☆—☆	30.	0.500 Lying
◇—◇	40.	0.500 Lying
▷—▷	50.	0.500 Lying
◻—◻	60.	0.500 Lying
◊—◊	70.	0.500 Lying
◌—◌	80.	0.500 Lying
◐—◐	85.	0.500 Lying
Ref.	Match	0.000 Flush

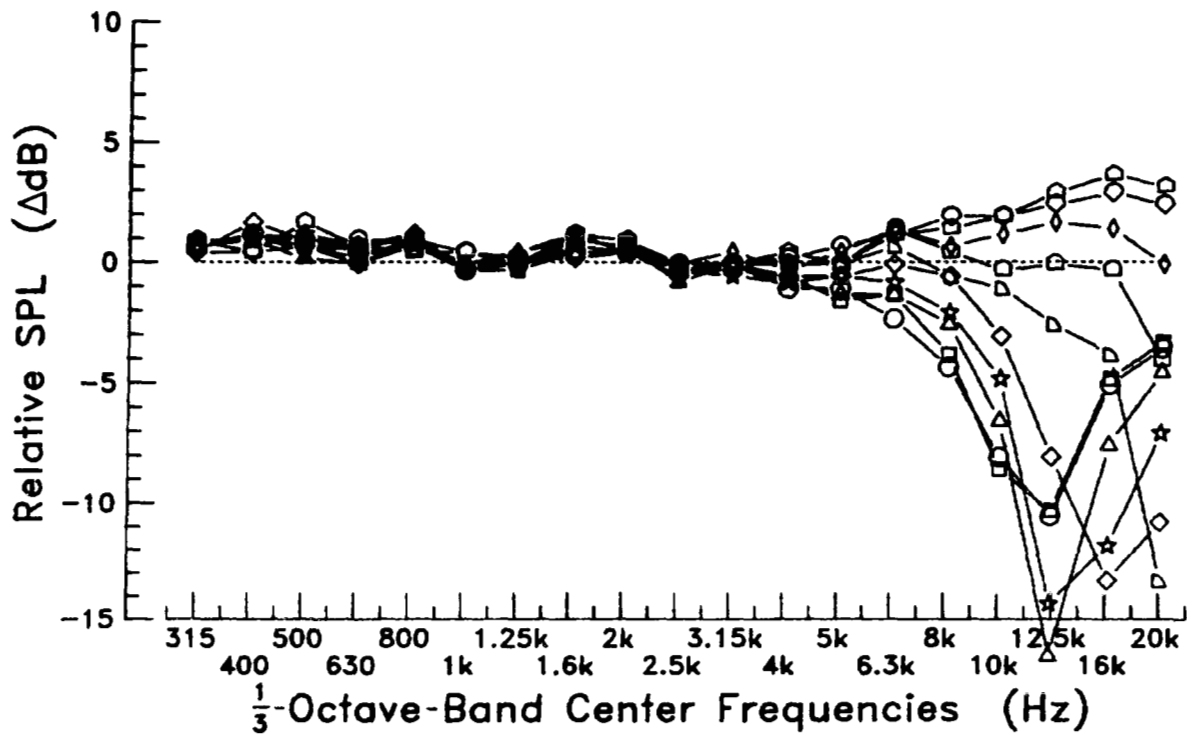


Figure 15.- Lying microphone versus flush-mounted microphone.

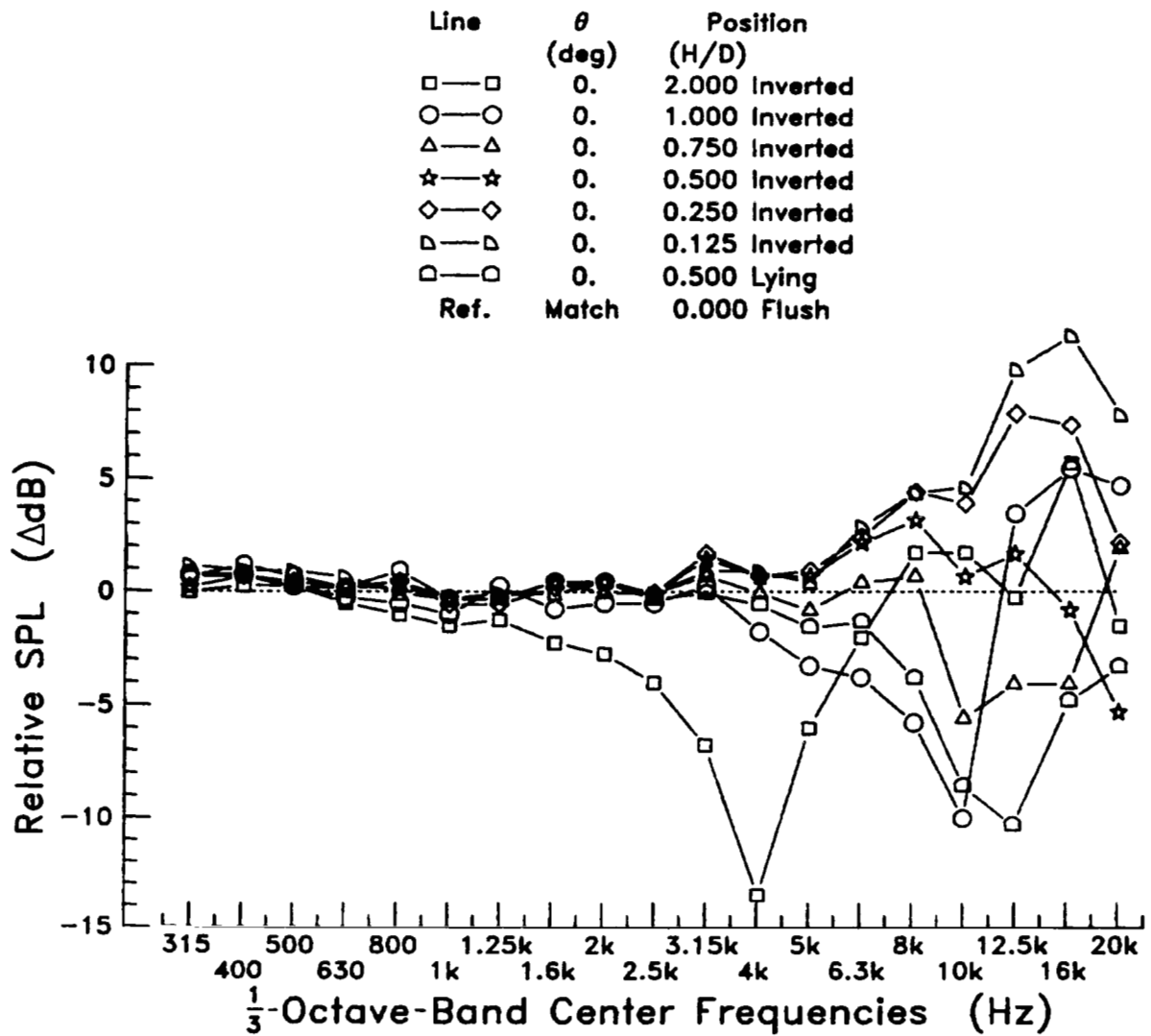


Figure 16.- All microphones at $\theta = 0^\circ$ versus flush-mounted microphone.

Line	θ (deg)	Position (H/D)
□—□	10.	2.000 Inverted
○—○	10.	1.000 Inverted
△—△	10.	0.750 Inverted
☆—☆	10.	0.500 Inverted
◇—◇	10.	0.250 Inverted
▷—▷	10.	0.125 Inverted
◻—◻	10.	0.500 Lying
Ref.	Match	0.000 Flush

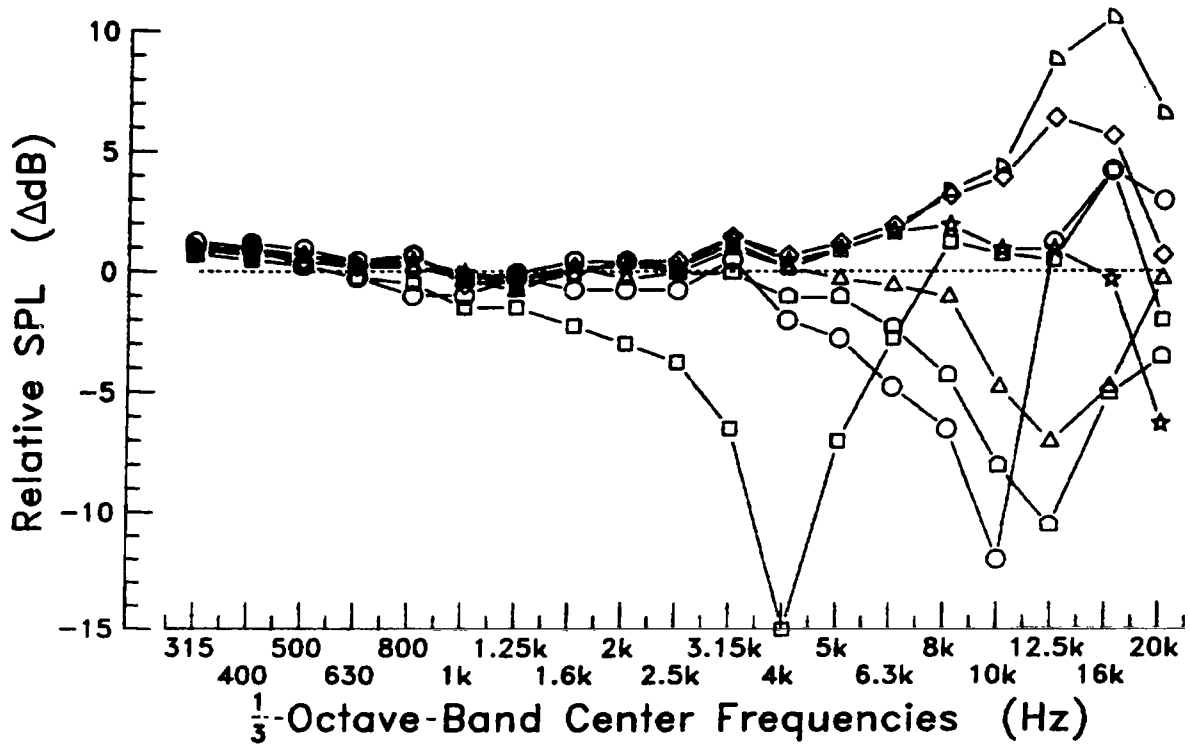


Figure 17.- All microphones at $\theta = 10^\circ$ versus flush-mounted microphone.

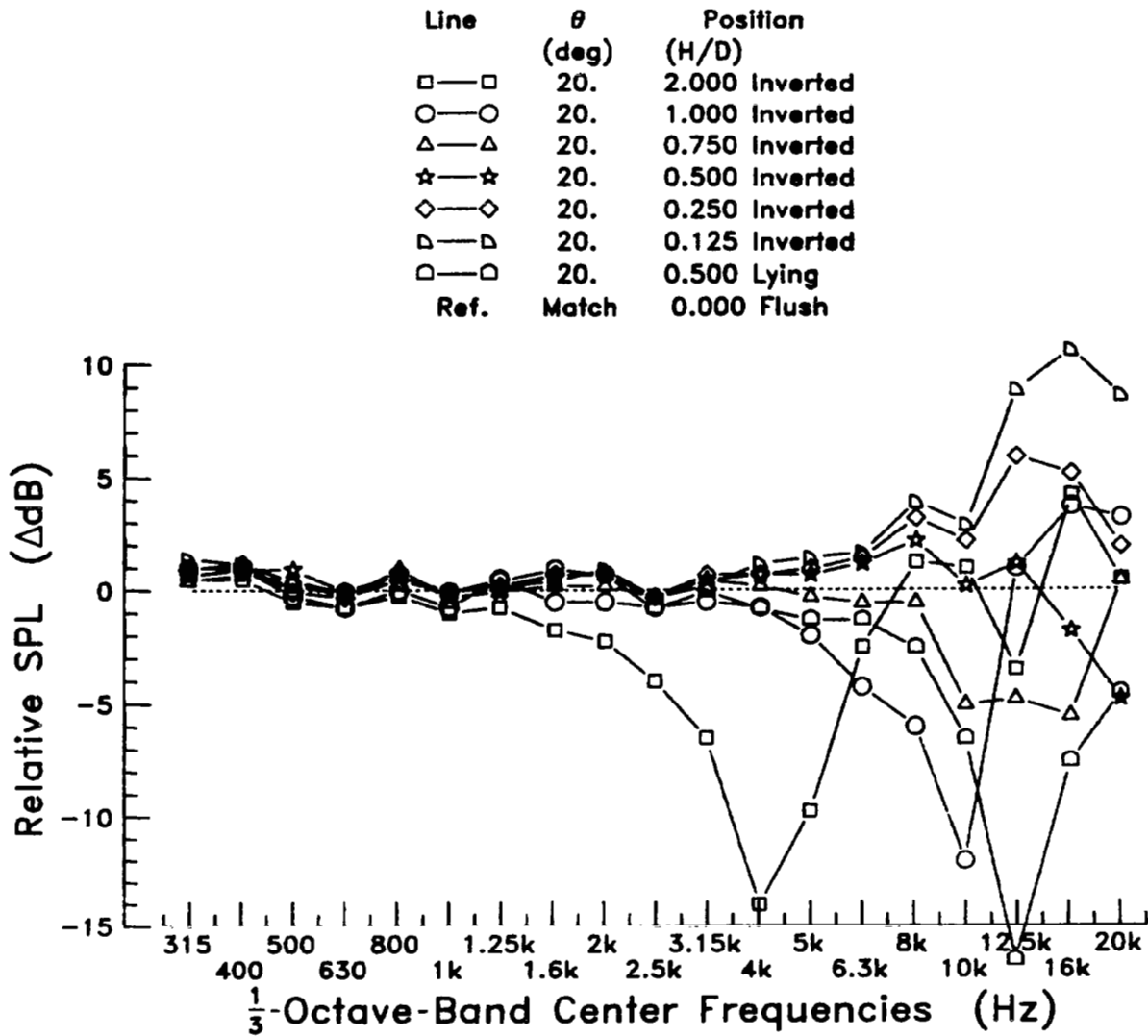


Figure 18.- All microphones at $\theta = 20^\circ$ versus flush-mounted microphone.

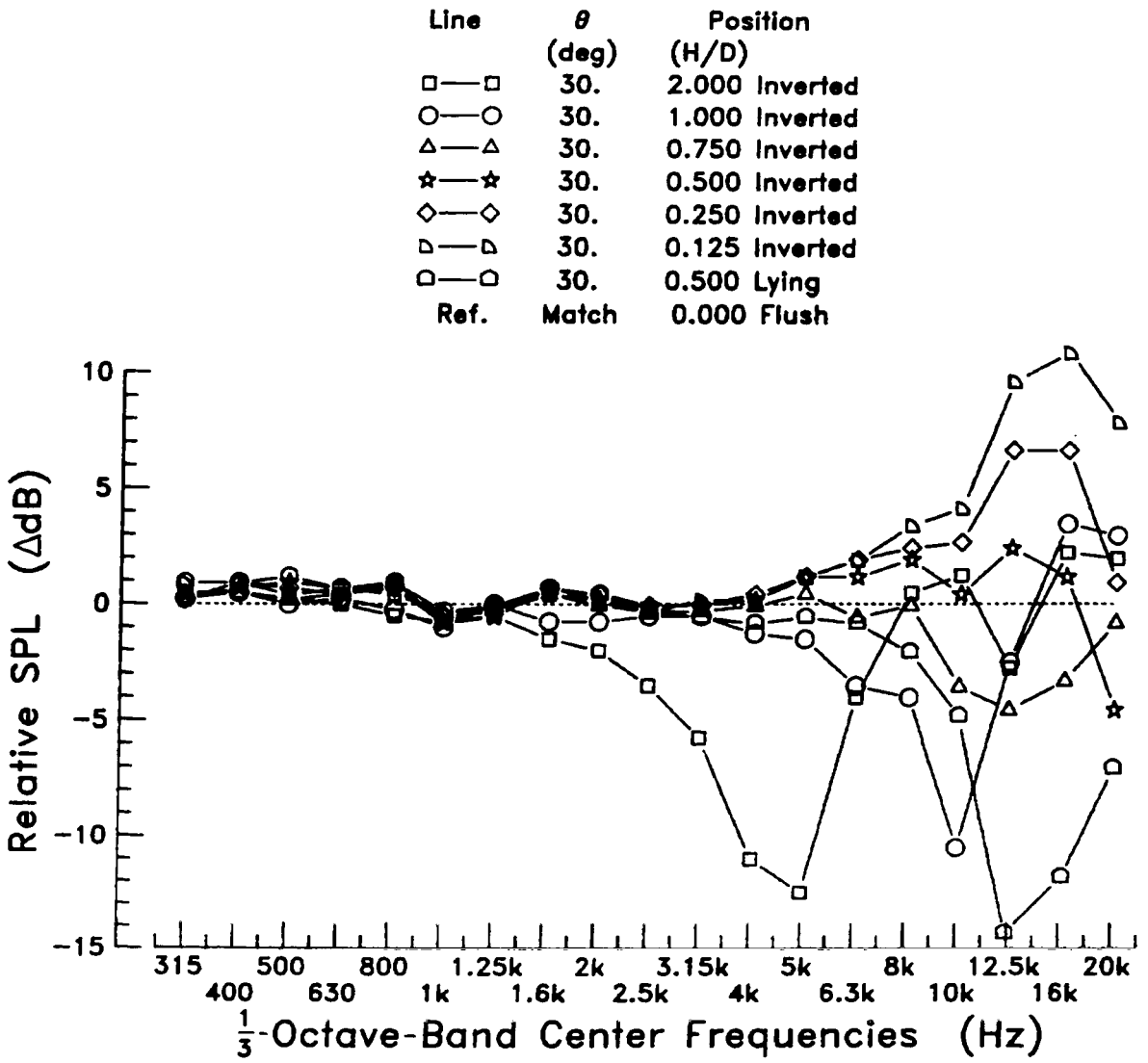


Figure 19.- All microphones at $\theta = 30^\circ$ versus flush-mounted microphone.

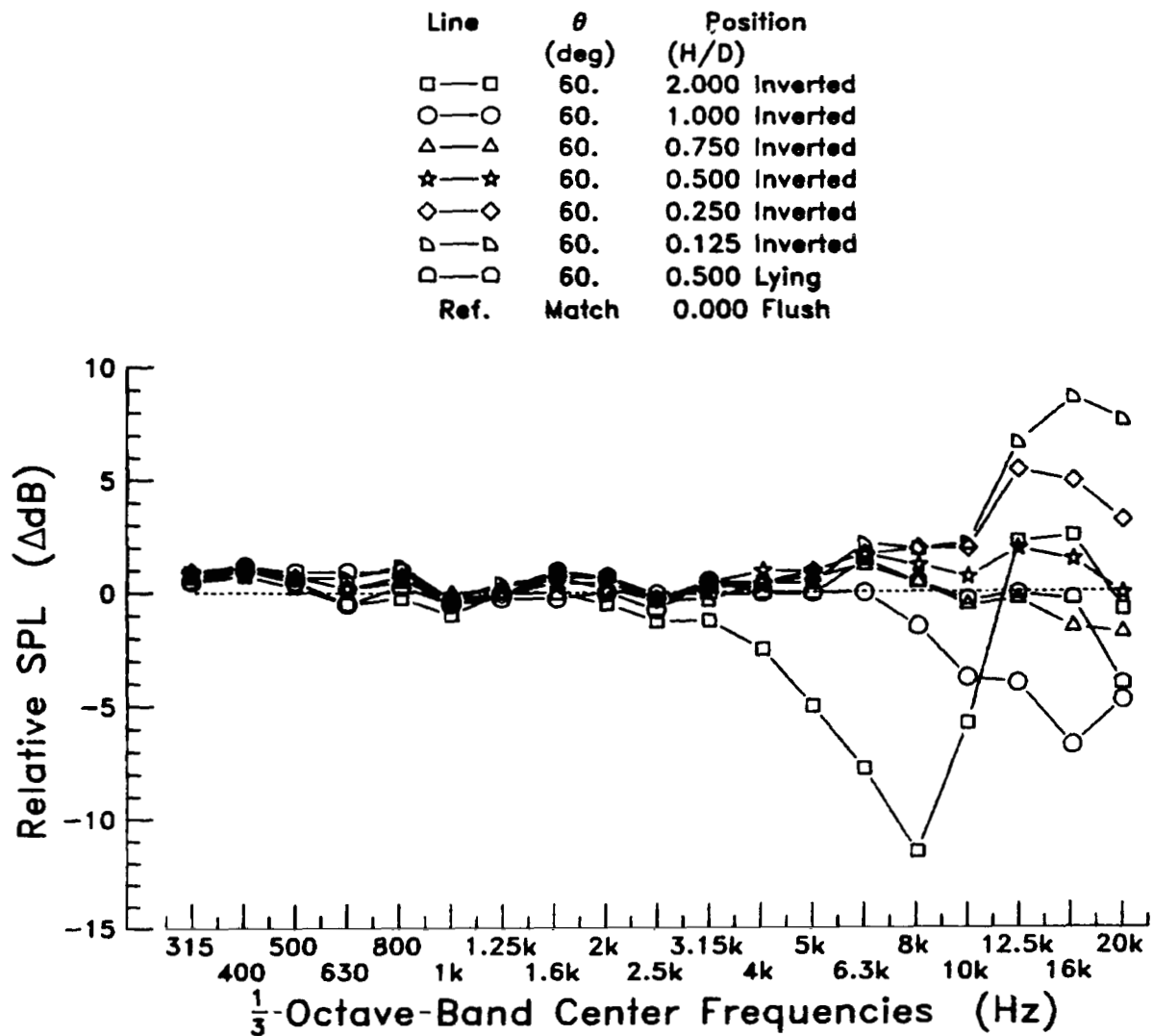


Figure 20.- All microphones at $\theta = 60^\circ$ versus flush-mounted microphone.

Line	θ (deg)	Position (H/D)
□—□	70.	2.000 Inverted
○—○	70.	1.000 Inverted
△—△	70.	0.750 Inverted
☆—☆	70.	0.500 Inverted
◇—◇	70.	0.250 Inverted
▷—▷	70.	0.125 Inverted
◻—◻	70.	0.500 Lying
Ref.	Match	0.000 Flush

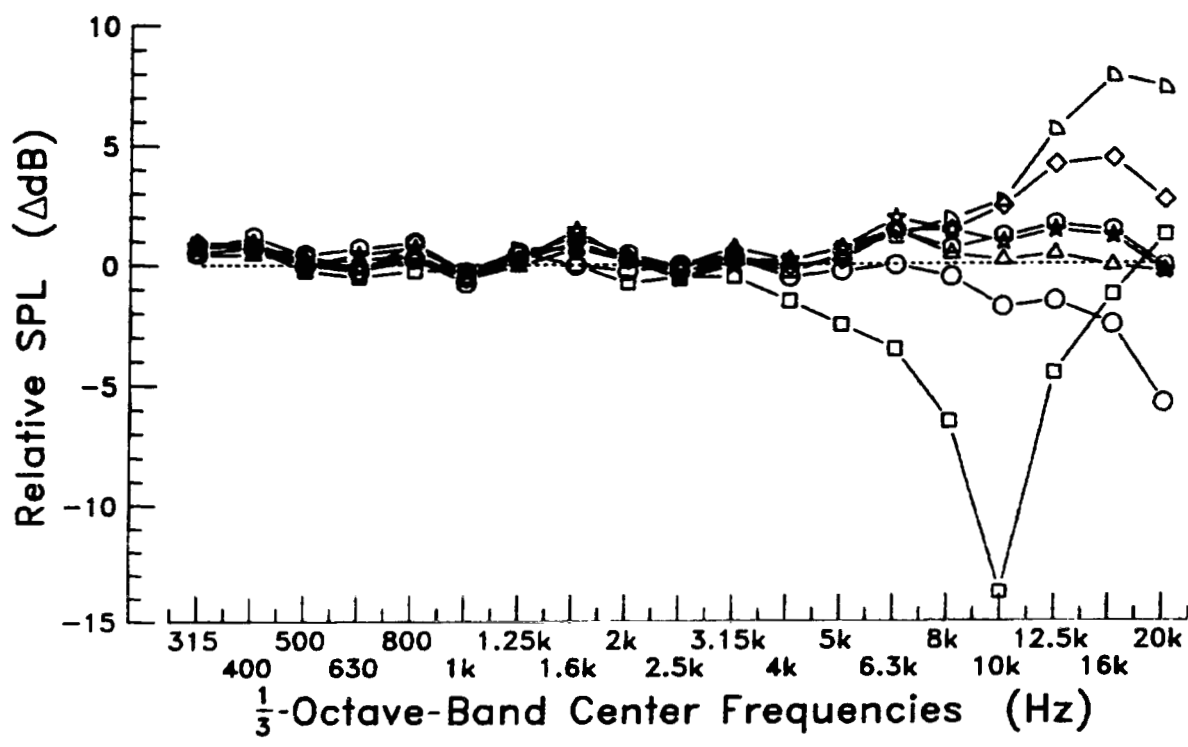


Figure 21.- All microphones at $\theta = 70^\circ$ versus flush-mounted microphone.

Line	θ (deg)	Position (H/D)
□—□	75.	2.000 Inverted
○—○	75.	1.000 Inverted
△—△	75.	0.750 Inverted
☆—☆	75.	0.500 Inverted
◇—◇	75.	0.250 Inverted
▷—▷	75.	0.125 Inverted
◻—◻	75.	0.500 Lying
Ref.	Match	0.000 Flush

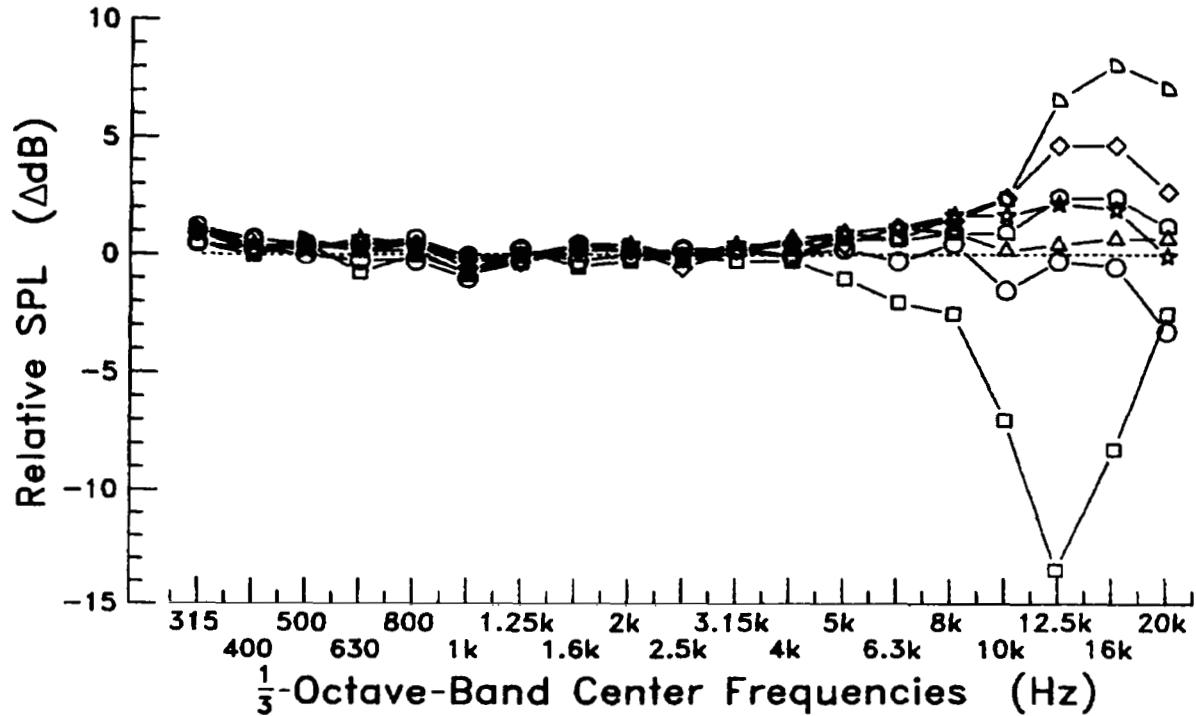


Figure 22.- All microphones at $\theta = 75^\circ$ versus flush-mounted microphone.

Line	θ (deg)	Position (H/D)
□—□	80.	2.000 Inverted
○—○	80.	1.000 Inverted
△—△	80.	0.750 Inverted
☆—☆	80.	0.500 Inverted
◇—◇	80.	0.250 Inverted
▷—▷	80.	0.125 Inverted
◻—◻	80.	0.500 Lying
Ref.	Match	0.000 Flush

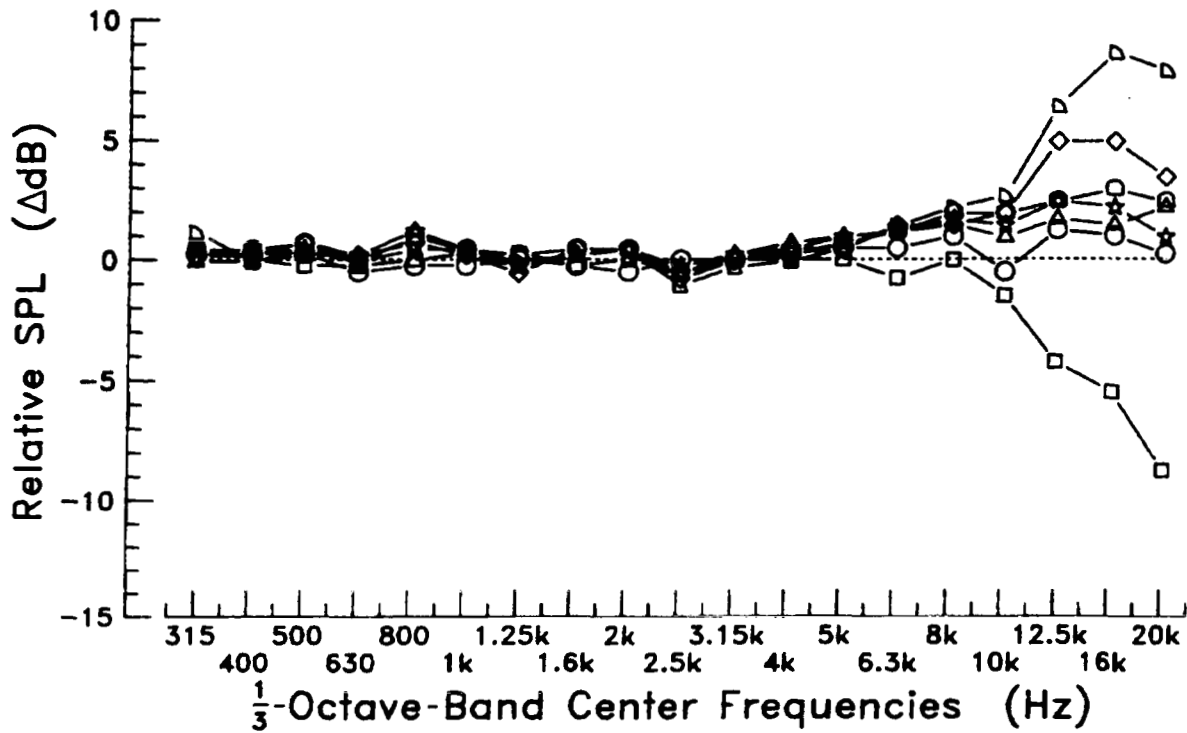


Figure 23.- All microphones at $\theta = 80^\circ$ versus flush-mounted microphone.

Line	θ (deg)	Position (H/D)
□—□	85.	2.000 Inverted
○—○	85.	1.000 Inverted
△—△	85.	0.750 Inverted
☆—☆	85.	0.500 Inverted
◇—◇	85.	0.250 Inverted
▷—▷	85.	0.125 Inverted
◻—◻	85.	0.500 Lying
Ref.	Match	0.000 Flush

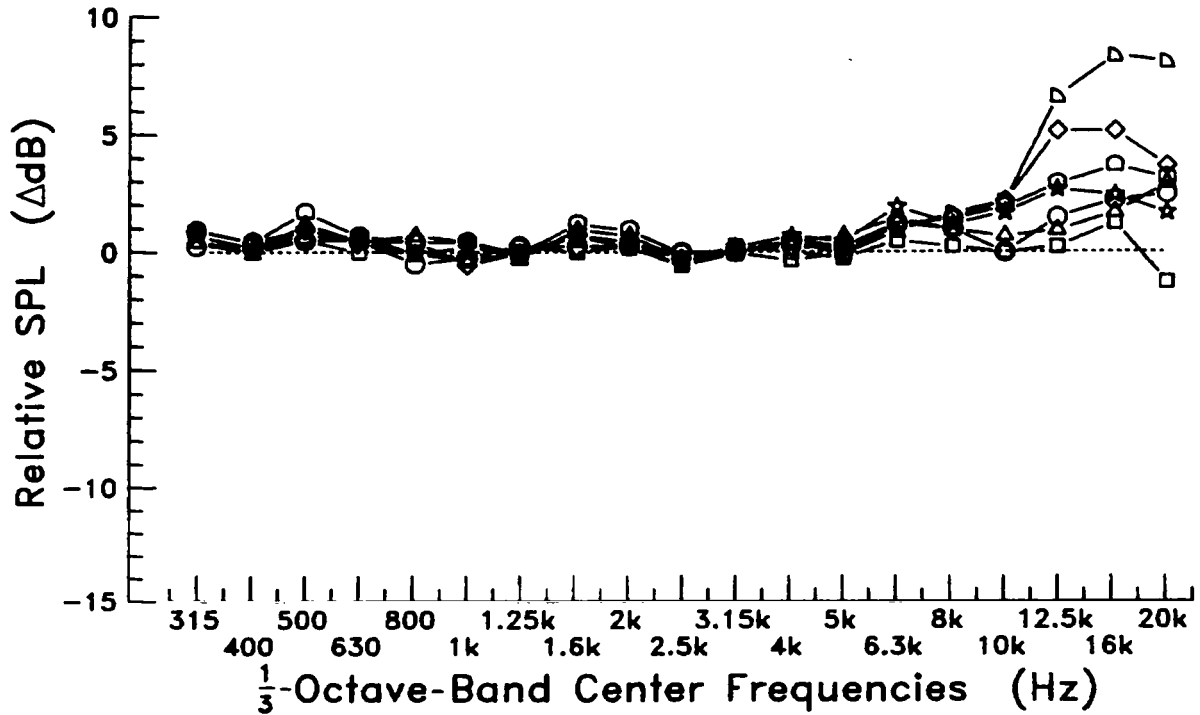


Figure 24.- All microphones at $\theta = 85^\circ$ versus flush-mounted microphone.

Line	θ (deg)	Position (H/D)
□—□	0.	2.000 Inverted
○—○	10.	2.000 Inverted
△—△	20.	2.000 Inverted
☆—☆	30.	2.000 Inverted
◇—◇	40.	2.000 Inverted
▷—▷	50.	2.000 Inverted
◻—◻	60.	2.000 Inverted
◊—◊	70.	2.000 Inverted
◌—◌	80.	2.000 Inverted
◐—◐	85.	2.000 Inverted
Ref.	Match	0.000 Flush

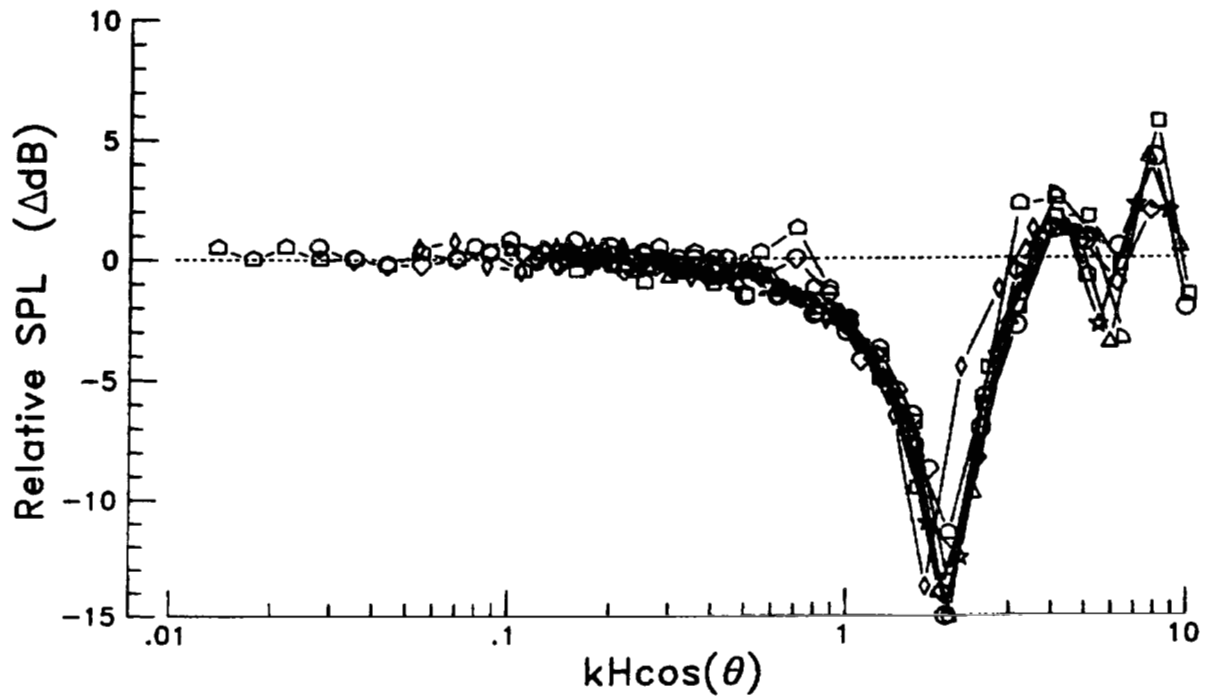


Figure 25.- Nondimensionalized inverted microphone for $H/D = 2$ versus flush-mounted microphone.

Line	θ (deg)	Position (H/D)
□—□	0.	1.000 Inverted
○—○	10.	1.000 Inverted
△—△	20.	1.000 Inverted
☆—☆	30.	1.000 Inverted
◇—◇	40.	1.000 Inverted
▷—▷	50.	1.000 Inverted
◻—◻	60.	1.000 Inverted
◊—◊	70.	1.000 Inverted
◌—◌	80.	1.000 Inverted
◻—◻	85.	1.000 Inverted
Ref.	Match	0.000 Flush

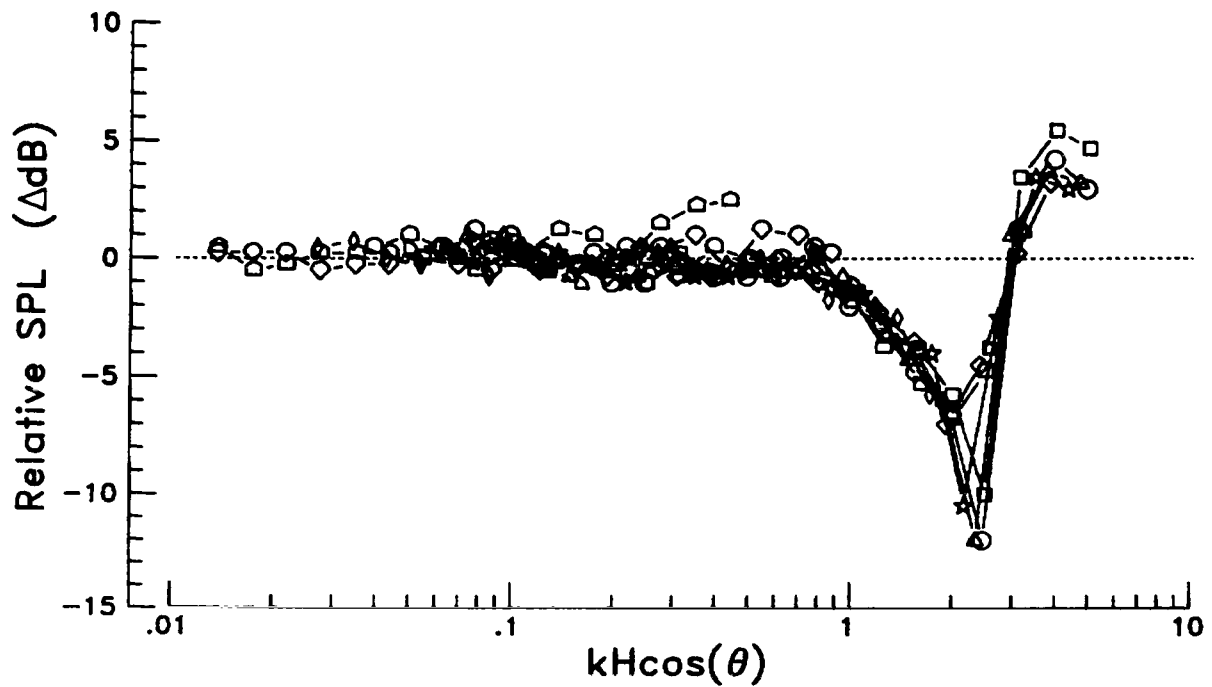


Figure 26.- Nondimensionalized inverted microphone for $H/D = 1$ versus flush-mounted microphone.

Line	θ (deg)	Position (H/D)
□—□	0.	0.750 Inverted
○—○	10.	0.750 Inverted
△—△	20.	0.750 Inverted
☆—☆	30.	0.750 Inverted
◇—◇	40.	0.750 Inverted
▷—▷	50.	0.750 Inverted
◻—◻	60.	0.750 Inverted
◊—◊	70.	0.750 Inverted
◌—◌	80.	0.750 Inverted
◑—◑	85.	0.750 Inverted
Ref.	Match	0.000 Flush

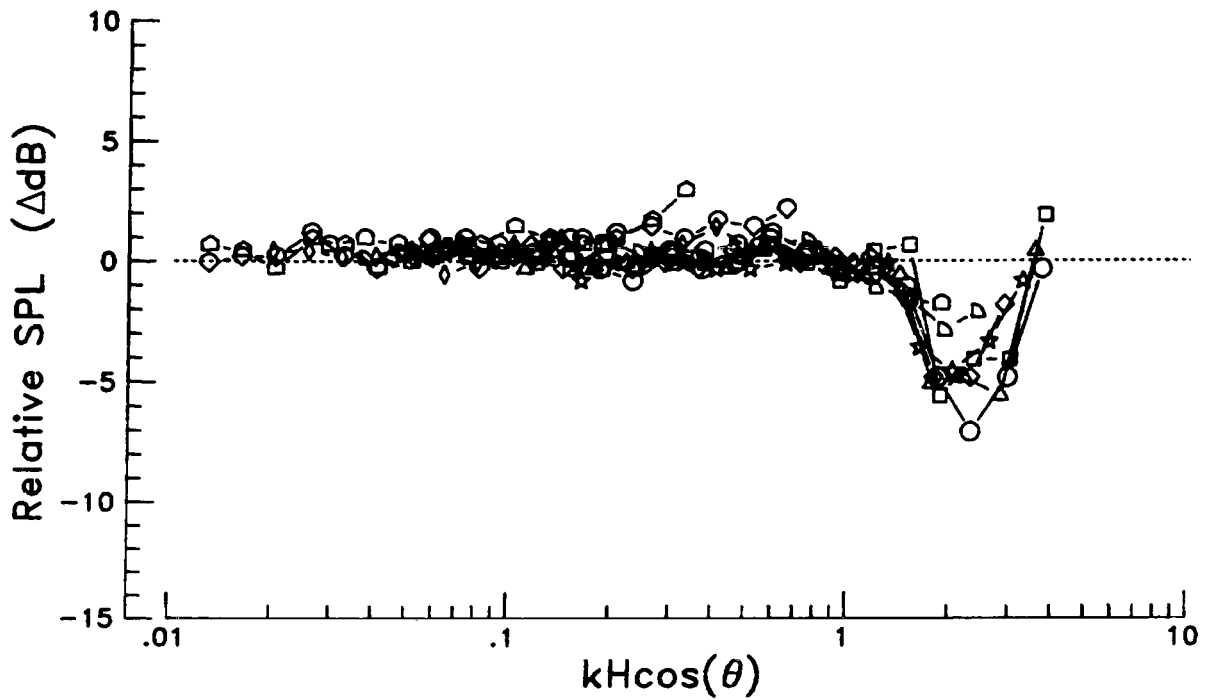


Figure 27.- Nondimensionalized inverted microphone for $H/D = 0.75$ versus flush-mounted microphone.

Line	θ (deg)	Position (H/D)
□—□	0.	0.500 Inverted
○—○	10.	0.500 Inverted
△—△	20.	0.500 Inverted
☆—☆	30.	0.500 Inverted
◇—◇	40.	0.500 Inverted
▷—▷	50.	0.500 Inverted
◻—◻	60.	0.500 Inverted
◊—◊	70.	0.500 Inverted
◈—◈	80.	0.500 Inverted
◑—◑	85.	0.500 Inverted
Ref.	Match	0.000 Flush

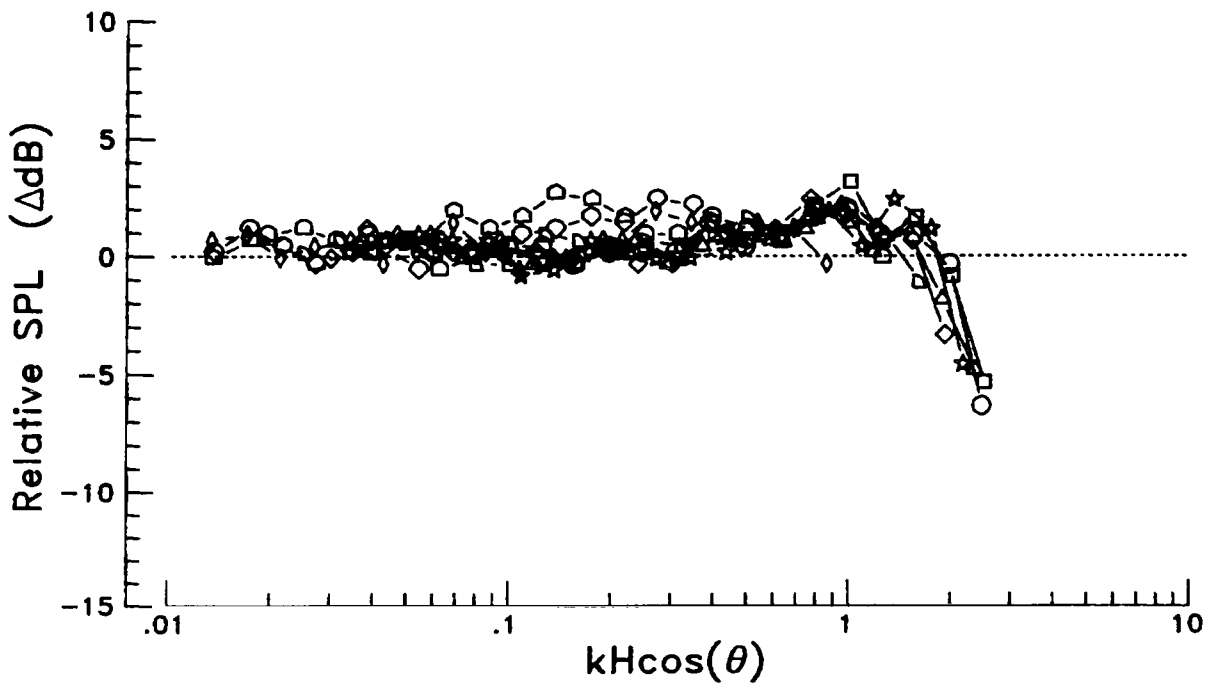


Figure 28.- Nondimensionalized inverted microphone for $H/D = 0.50$ versus flush-mounted microphone.

Line	θ (deg)	Position (H/D)
□—□	0.	0.250 Inverted
○—○	10.	0.250 Inverted
△—△	20.	0.250 Inverted
☆—☆	30.	0.250 Inverted
◇—◇	40.	0.250 Inverted
▷—▷	50.	0.250 Inverted
◻—◻	60.	0.250 Inverted
◊—◊	70.	0.250 Inverted
◌—◌	80.	0.250 Inverted
◑—◑	85.	0.250 Inverted
Ref.	Match	0.000 Flush

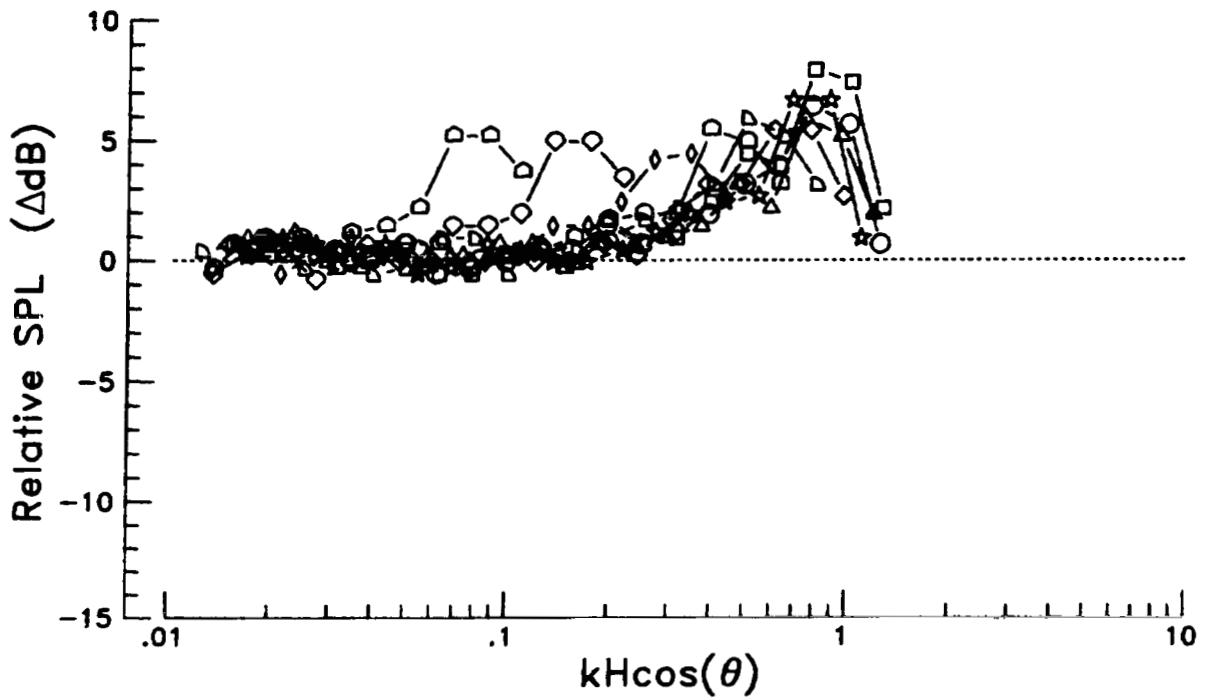


Figure 29.- Nondimensionalized inverted microphone for $H/D = 0.25$ versus flush-mounted microphone.

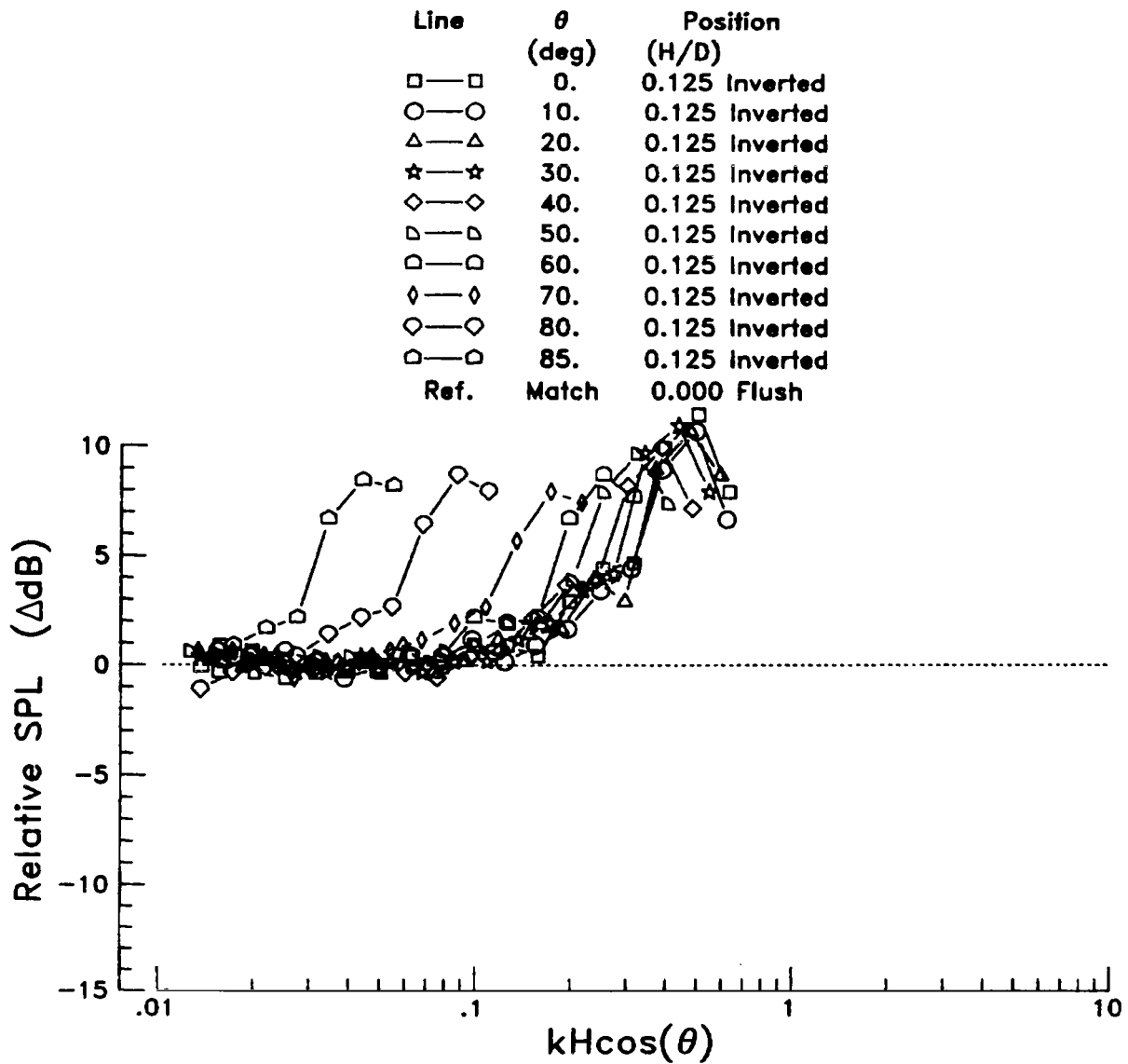


Figure 30.- Nondimensionalized inverted microphone for $H/D = 0.125$ versus flush-mounted microphone.

Line	θ (deg)	Position (H/D)
□—□	0.	0.500 Lying
○—○	10.	0.500 Lying
△—△	20.	0.500 Lying
☆—☆	30.	0.500 Lying
◇—◇	40.	0.500 Lying
▷—▷	50.	0.500 Lying
◻—◻	60.	0.500 Lying
◊—◊	70.	0.500 Lying
◌—◌	80.	0.500 Lying
◡—◡	85.	0.500 Lying
Ref.	Match	0.000 Flush

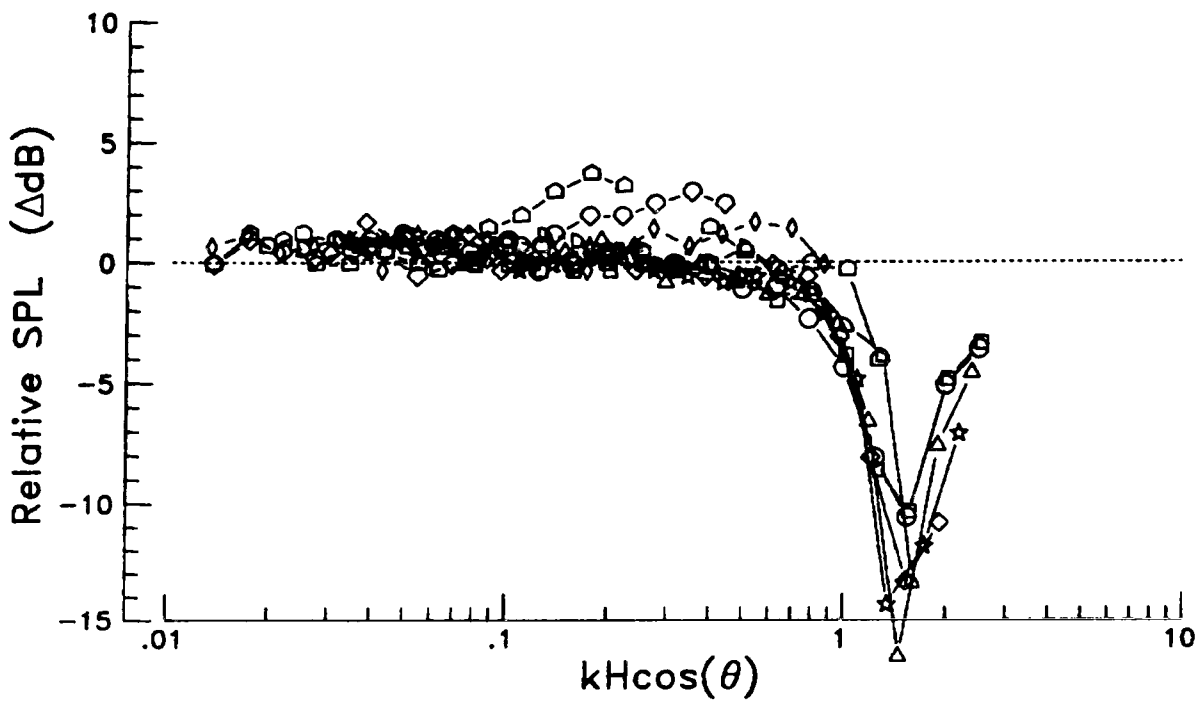


Figure 31.- Nondimensionalized lying microphone versus flush-mounted microphone.

1. Report No. NASA TP-2004		2. Government Accession No.		3. Recipient's Catalog No.	
4. Title and Subtitle INVESTIGATION OF EFFECTS OF MICROPHONE POSITION AND ORIENTATION ON NEAR-GROUND NOISE MEASUREMENTS				5. Report Date April 1982	
7. Author(s) William L. Willshire, Jr., and Paul A. Nystrom				6. Performing Organization Code 505-32-03-01	
9. Performing Organization Name and Address NASA Langley Research Center Hampton, VA 23665				8. Performing Organization Report No. L-15097	
12. Sponsoring Agency Name and Address National Aeronautics and Space Administration Washington, DC 20546				10. Work Unit No.	
15. Supplementary Notes				11. Contract or Grant No.	
16. Abstract Three ground-level-microphone mounting techniques (flush mounting, inverting the microphone over a plate, and lying the microphone on a plate) were compared over a frequency range from 315 Hz to 20 kHz and over a wide range of incidence angles in the Langley Jet-Noise Laboratory anechoic room. The flush-mounted microphone, when compared with a free-field microphone, exhibited approximate pressure doubling up to a frequency of 10 kHz. At frequencies less than 4 kHz, the inverted and lying microphones were in good agreement with the flush-mounted microphone, and their 1/3-octave-band response spectra were fairly insensitive to the position of the microphone. At higher frequencies, the geometry of the microphone and its mounting became important. The inverted microphone 0.5 times the diameter above the plate gave the flattest response compared with the flush-mounted microphone. Nondimensional analysis of the inverted and lying results showed that for $kH \cos \theta < 0.7$ the response of the microphones approached that of the flush-mounted microphone.				13. Type of Report and Period Covered Technical Paper	
17. Key Words (Suggested by Author(s)) Acoustics Ground-level microphone Microphone mounting techniques				14. Sponsoring Agency Code	
18. Distribution Statement Unclassified - Unlimited Subject Category 71					
19. Security Classif. (of this report) Unclassified	20. Security Classif. (of this page) Unclassified	21. No. of Pages 43	22. Price A03		

National Aeronautics and
Space Administration

Washington, D.C.
20546

Official Business

Penalty for Private Use, \$300

THIRD-CLASS BULK RATE

Postage and Fees Paid
National Aeronautics and
Space Administration
NASA-451



1 1 1971, 04152 50070303
DEPT OF THE AIR FORCE
AF WEAPONS LABORATORY
ATTN: TECHNICAL LIBRARY (S-11)
WRIGHT PATTENSON AIR FORCE BASE
DAYTON OH 45433



POSTMASTER: If Undeliverable (Section 158
Postal Manual) Do Not Return